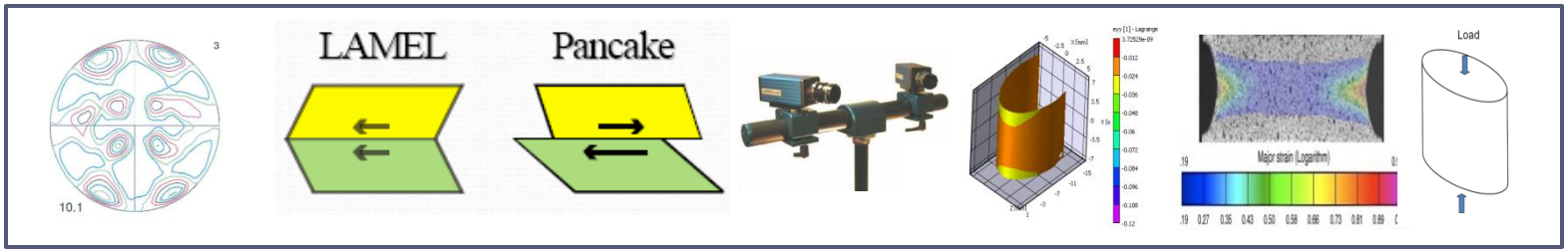

Identification and validation of CRSS values for Ti_6Al_4V alloy

W Hammami, G. Gilles, V. Tuninetti, L. Duchêne, AM Habraken

*L. Delannay **UCL** Louvain La Neuve Be*
*S. Bouvier **Labo Robertval** Compiègne Fr*
*B. Bacroix, Thierry Chauveau **Paris 13** Fr*
*E. Hug **CRISMAT** Caen Fr*

Plasticity 2013, Bahamas, Symposium to honour Paul Van Houtte

Replace mechanic EP macroscopic phenomenological models by microscopic one.

Why?

More physical roots

→**Able to represent strain paths not used for identification**

→Less number of material parameters to identify

Doubts

→Microstructure (grain size, texture, precipitates, phase)

X Ray, EBSD, SEM → less expensive ?
→ quicker ?

OK if material complexity does not make it mandatory that the model forgets key mechanism

→**Less parameters to fit or identify, generic ones in literature?**

*Not convinced 35 parameters in crystal gradient plasticity based on **G**eometrically **N**ecessary **Di**slocations and **S**tatisticall **S**tored **D**islocations on pure Nickel (single phase materials...)*

Keller; Hug; Habraken et al *IJP* (2012) 29

Keller, Habraken, Duchêne *Mat Sc & Eng A* (2012), 550(30),

Be reasonable

Find a good compromise

Let just the Macro and Micro worlds try to be complementary

Let us try to play the game …

A single Ti_6Al_4V sheet material

- ***Experimental data base :***
  monotonic tests (tensile, plane strain, compression, shear) + Baushinger shear tests + cup deep drawing

- ***Crystal Plasticity Model***
  Identify Critical Resolved Shear Stress on some tests

- ***Phenomenological Cazacu Model***
  Identify a set of material parameters on some tests

- ***Check validity on other type of strain paths***

- ***Compare predictions***

Chosen Ti_6Al_4V Sheet

Hot and cold rolling followed by one hour of mill annealing at 760 C

Thickness : 0.6mm

Phases: HCP α phase, BCC β Phase

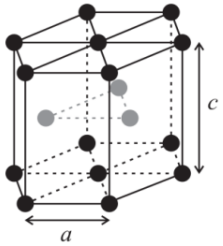

Alpha phase: 88.2%

Beta phase: 9.3%

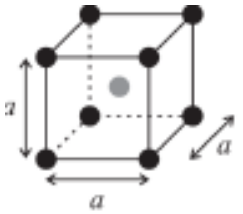

Grain size: 2.24 µm α phase

β phase < 1 µm inlayed between grains boundaries of the α-phase

Chemical component	Ti [%]	Al [%]	V [%]	O [%]	N [ppm]	C [ppm]	H [ppm]	Fe [%]
Top	Bal.	6.22	3.93	0.19	60	80	100	0.16
Bottom	Bal.	6.27	4	0.20	60	90	86	0.16

Initial Texture

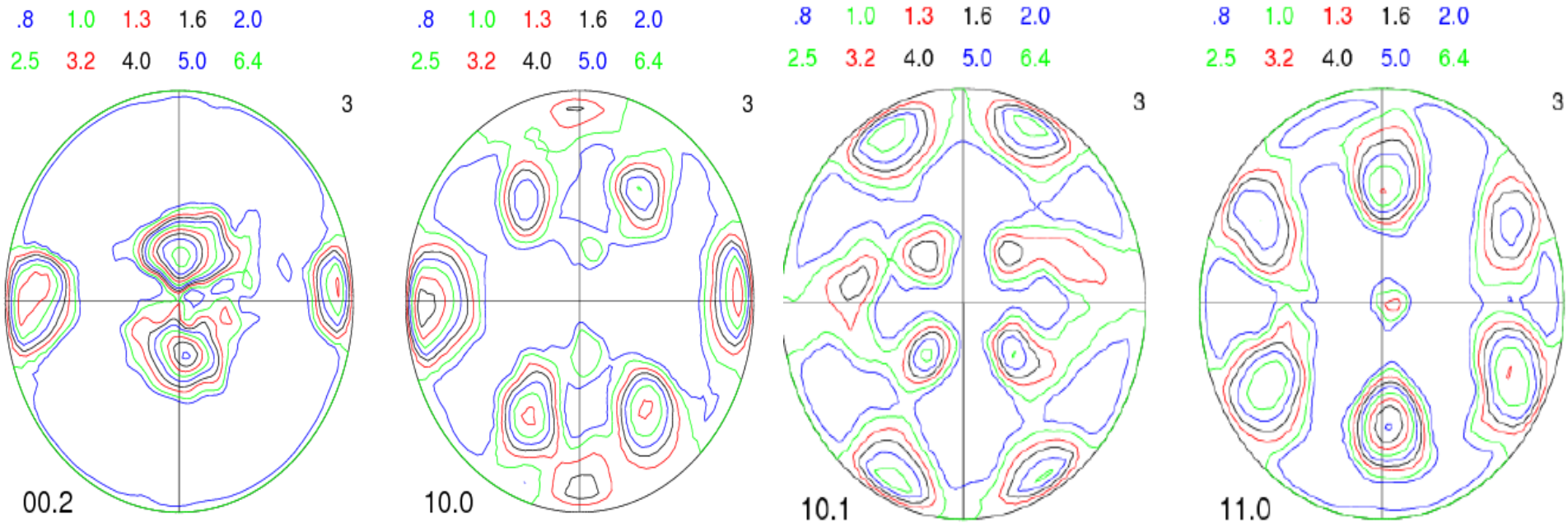

C axis oriented along (TD)
or 13 ND in the plane RD ND

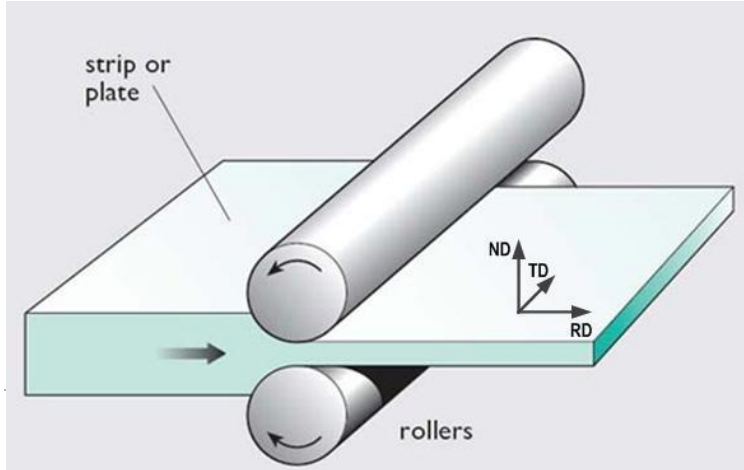

Plastic Deformation by dislocation slips along slip system families

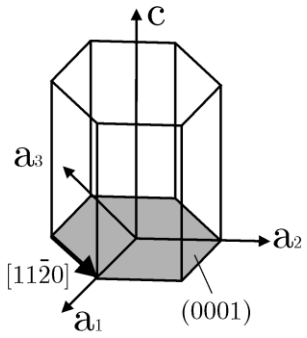

Basal-<a>

(0001)<11$\bar{2}$0>, 3

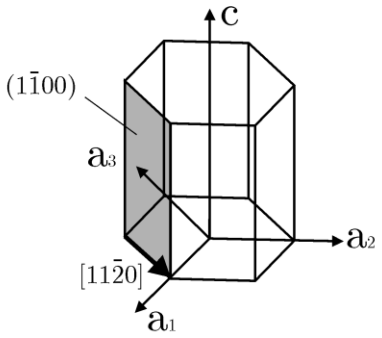

Prismatic-<a>

{10$\bar{1}$0}<11$\bar{2}$0>, 3

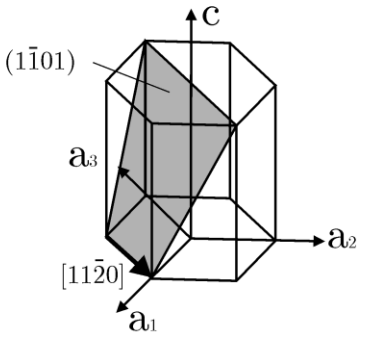

Pyramidal-<a>

{10$\bar{1}$1}<11$\bar{2}$0>, 6

Most densely populated lattice planes and directions

(here we keep only 24 systems)

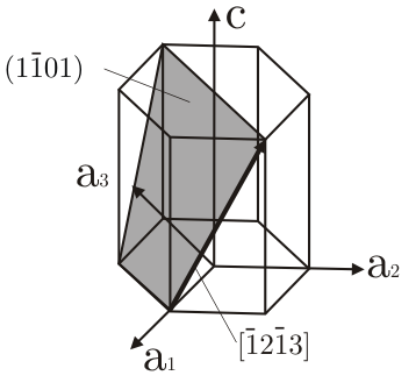

1st order

Pyramidal-<c+a>

{10$\bar{1}$1}<11$\bar{2}$3>, 12

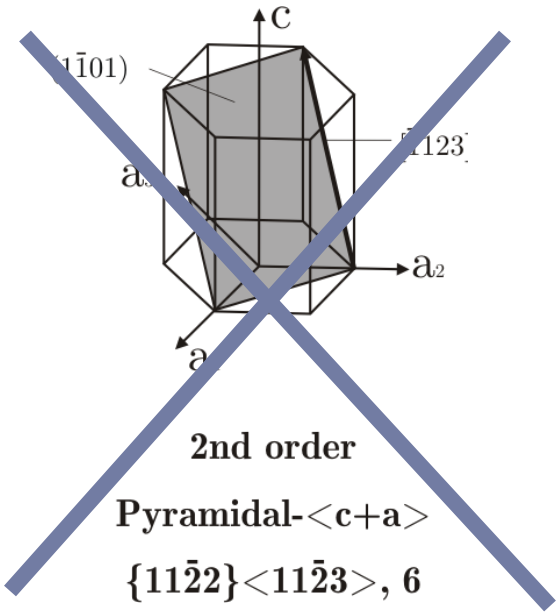

2nd order

Pyramidal-<c+a>

{11$\bar{2}$2}<11$\bar{2}$3>, 6

Ti_6Al_4V Critical Resolved Shear Stress

$\tau^{basal}_{CRSS}/\tau^{prism}_{CRSS}$	$\tau^{pyr\langle a\rangle}_{CRSS}/\tau^{prism}_{CRSS}$	$\tau^{pyr\langle c+a\rangle}_{CRSS}/\tau^{prism}_{CRSS}$		Reference
0.93–1.3	1	1.1–1.6	(Sachs)	Medina Perilla and Gil Sevillano (1995)
1.25	–	2.625		Paton et al. (1973)
5	5	8.0–15.0	(Sachs)	Fundenberger et al. (1997)
1.5	1	3		Dunst and Mecking (1996)
1	–	8	(Taylor)	Lebensohn and Canova (1997)
1.43	–	4.23		Bieler and Semiatin (2001)

J.R. Mayeur, D.L. McDowell,, *IJP* 2007, vol. 23, pp1457-1485.

1.53	1	7,03	(VPSC)	Coghe et al (P Van Houtte) *Mater Sci. Eng. A 537 (2012)*
1.05	-	1.6	(CPFEM)	Dick et al. *Comp Mater Sc.* (2006) 38

Dependence of model choice, of test used, of initial texture, thermal treatment on material….

Twinning in Ti_6Al_4V ?

no twins: effect of Al + second phase
Zaefferer *Mater Sci. Eng. A 344 (2003)*

some twins Xiao *Mater Sci. Eng. A 394 (2005)*

some twins + reorientation of complete grain parents
Prakash et al. *Mater Sci. Eng. A 527 (2010)*

high level of twins in Equal Channel Angular Extrusion
Yapici et al. *Acta Mater. 54 (2006)*

tensile twins in compression
Coghe et al *Mater Sci. Eng. A 537 (2012)*

Twinning ?

Pure HCP Ti, Mg, Zr, twinning = important mechanism

Twinning ↑→ strain hardening ↑with deformation

Barnett et al. *Scripta Mater* (2005) 52

$Ti_6 Al_4$ V bar
Compressed samples

Twin fraction
Initial < 1%

Final static test S

4.8 +- 1.7 %

Final dynamic test D

8.9 +- 2 %

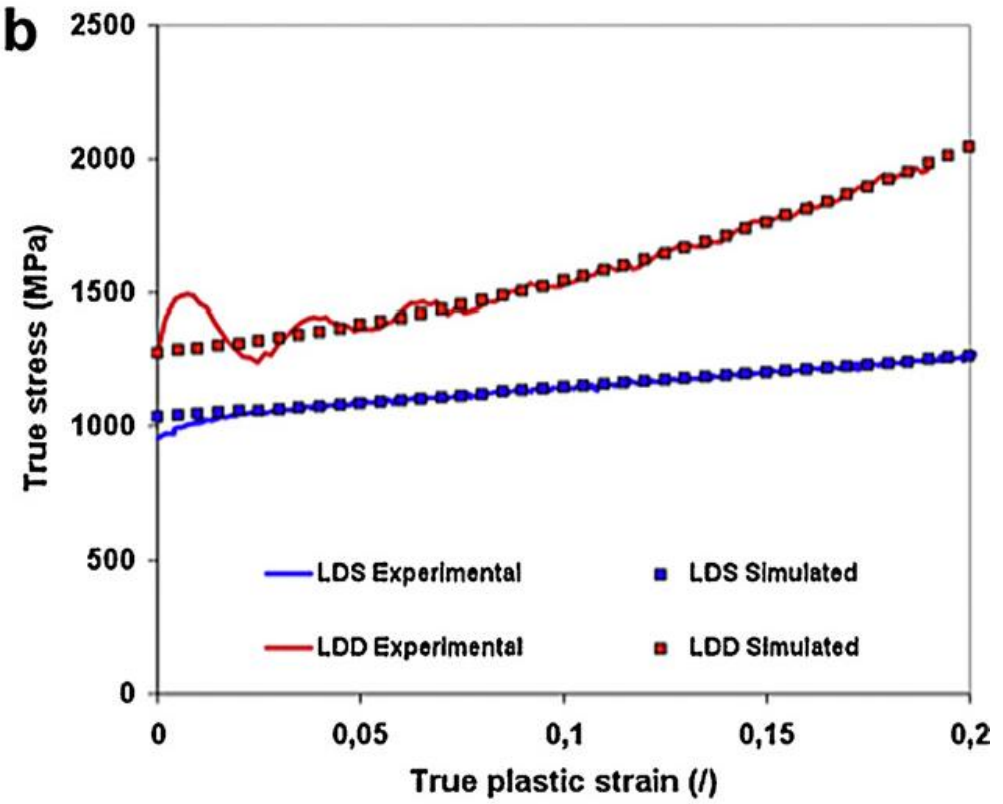

Dynamic compression tests: twinning justifies 30% of texture change

Coghe et al (P Van Houtte) *Mater Sci. Eng. A 537 (2012)*

Twinning in Ti_6Al_4V ?

Ti_6Al_4V tensile twins in compression up to 9 %

Coghe et al (P Van Houtte) *Mater Sci. Eng. A 537 (2012)*

texture evolution c axis ⊥ compression axis

→Lining up with compression direction, effect of tensile twins

→ Easy way to identify twins = check evolution of C axis

consistent observations through EBSD, TEM, Optic Microscopy + indentation to identify parent grain and twins

The smallest fraction in a grain not necessarily the twin variant...

twinning = not a complementary mechanism
= competing deformation mechanism
(final fraction 3 to 9 % according direction, static or dynamic tests)

In static tensile tests along TD direction, final twin fraction under 1%
Twinning can be neglected to predict stress strain curves

Twinning in our Ti_6Al_4V sheet ?

Compression, Shear test = biggest amount of twinning but still < 2.5 %

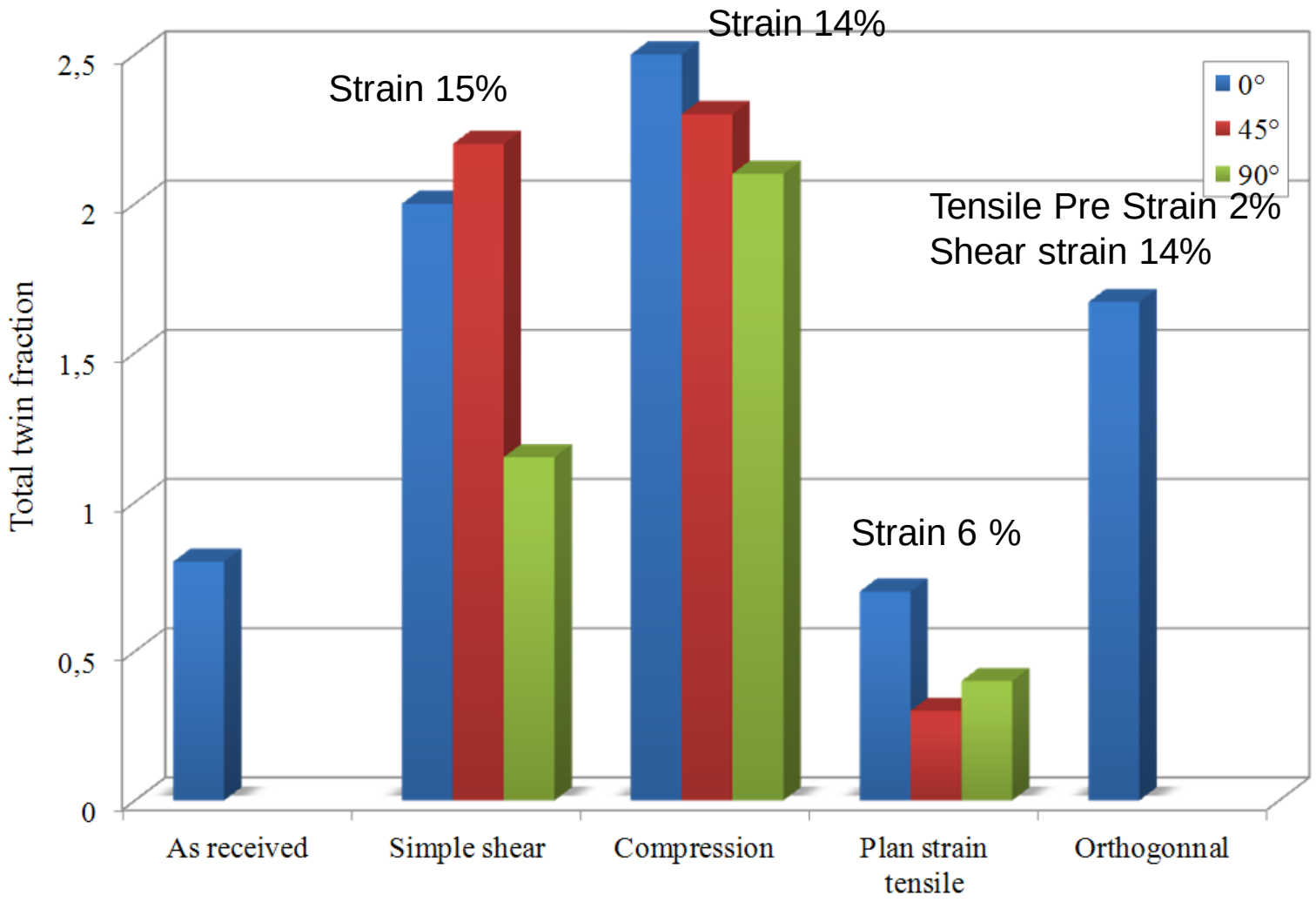

Is the hardening behavior a ‘twinning’ one ?

Focus on compression and shear tests

with the highest fraction of twinning ….

Compression in Kuwabara lab

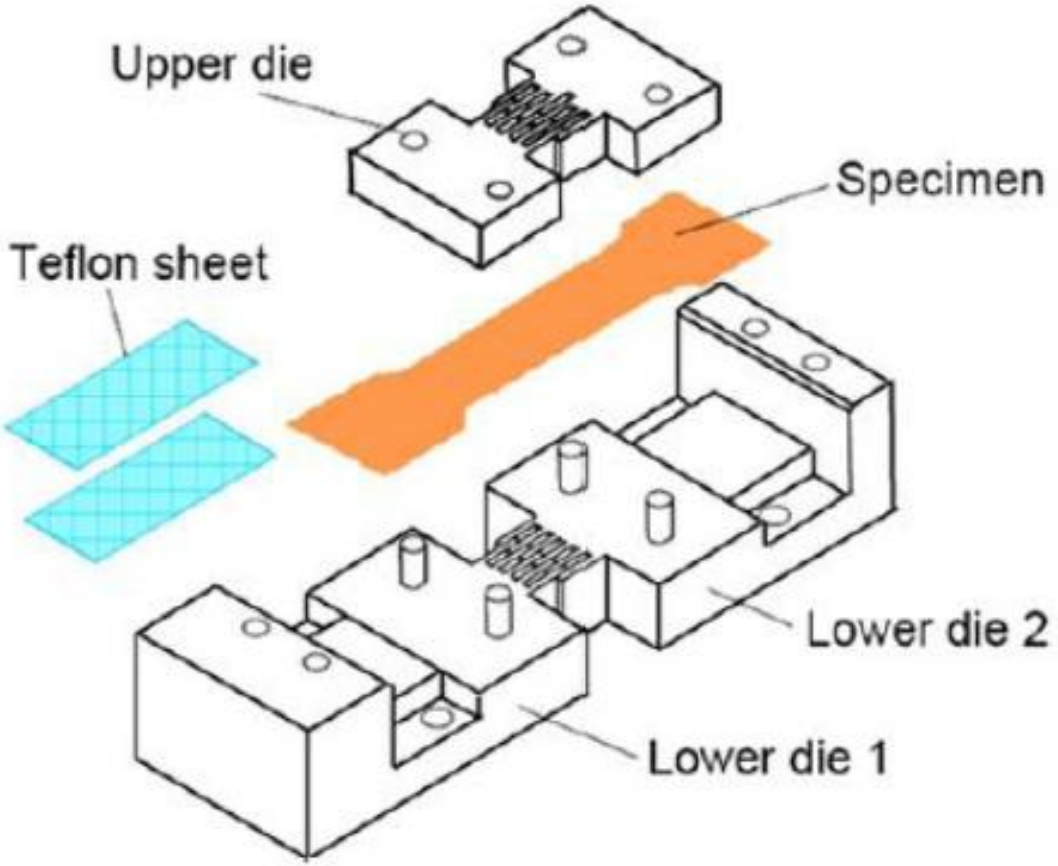

Kuwabara et al. IJP 2009 (25)

Compression results

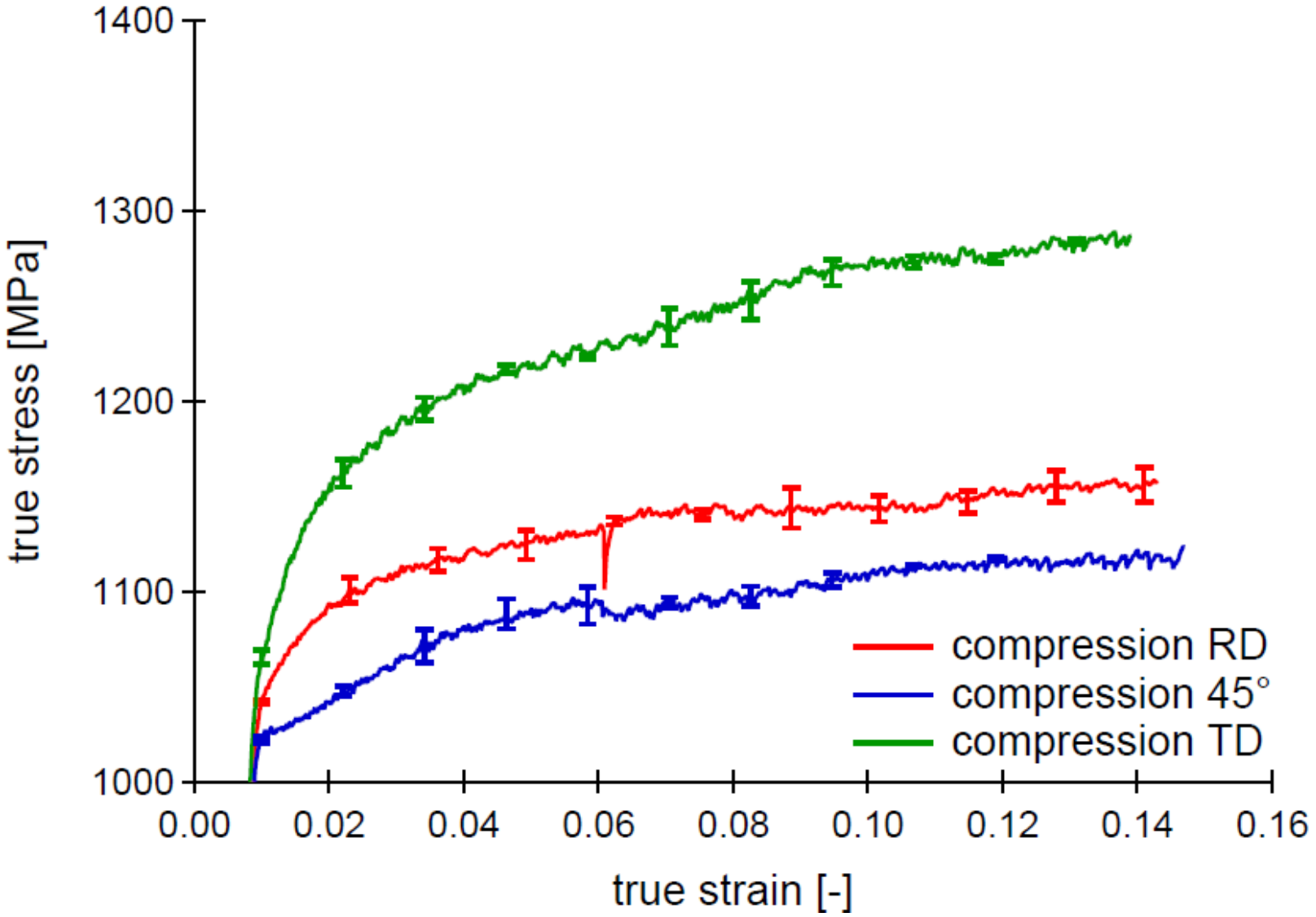

Simple shear in Ulg lab

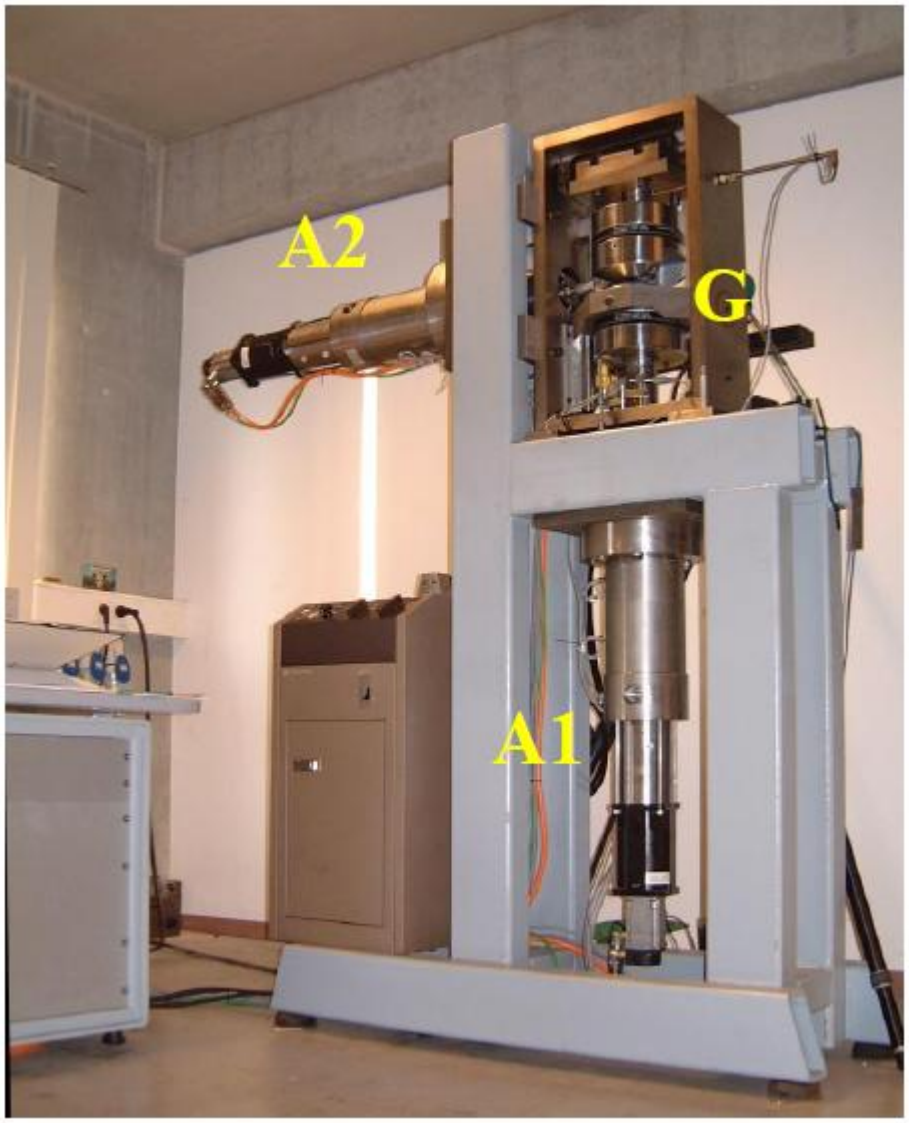

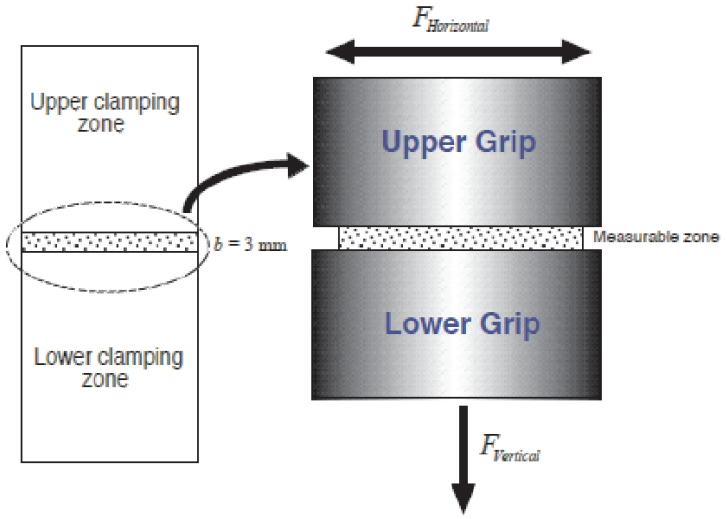

Bi axial machine used for

-Simple shear
monotonic or Baushinger
-Plane strain tests
-Orthogonal tests
-Simultaneous tests

Simple shear in Ulg lab

Shorter length and reduced size of gage zone

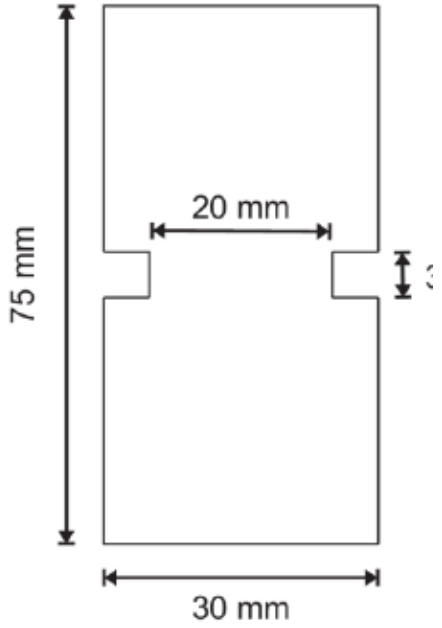

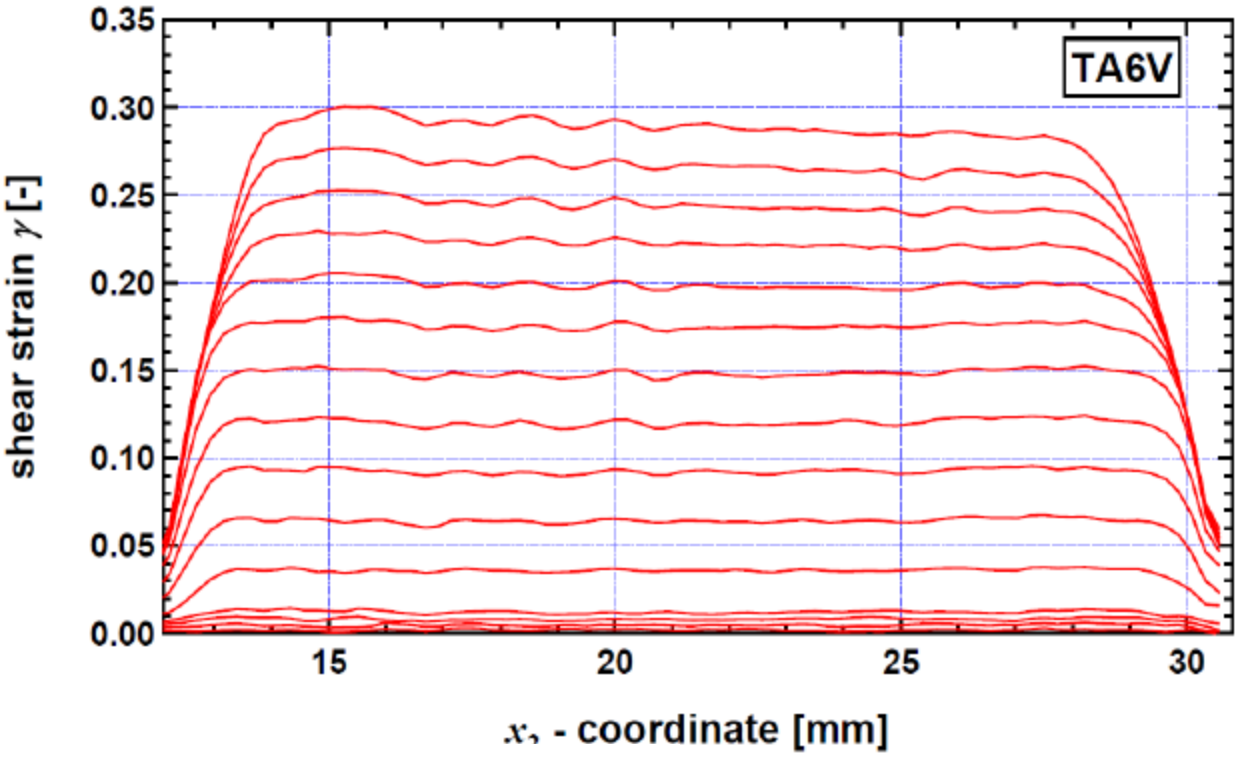

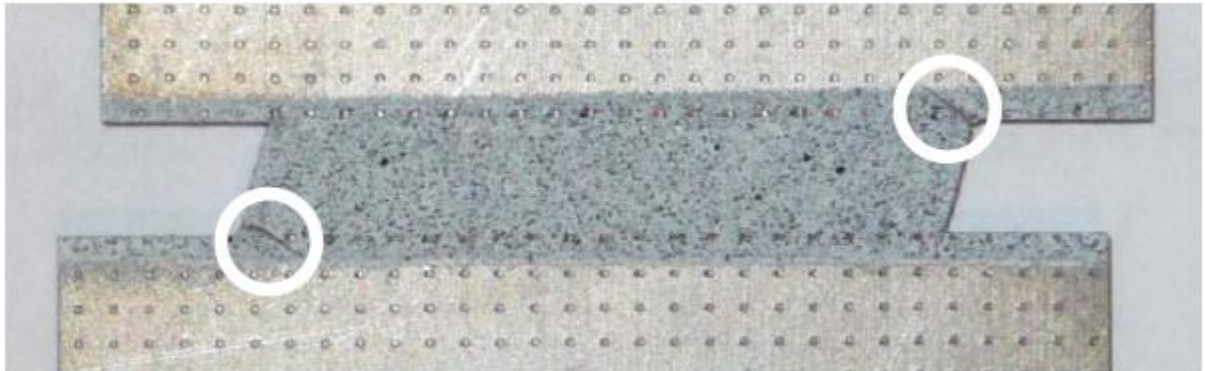

Simple shear in Ulg lab

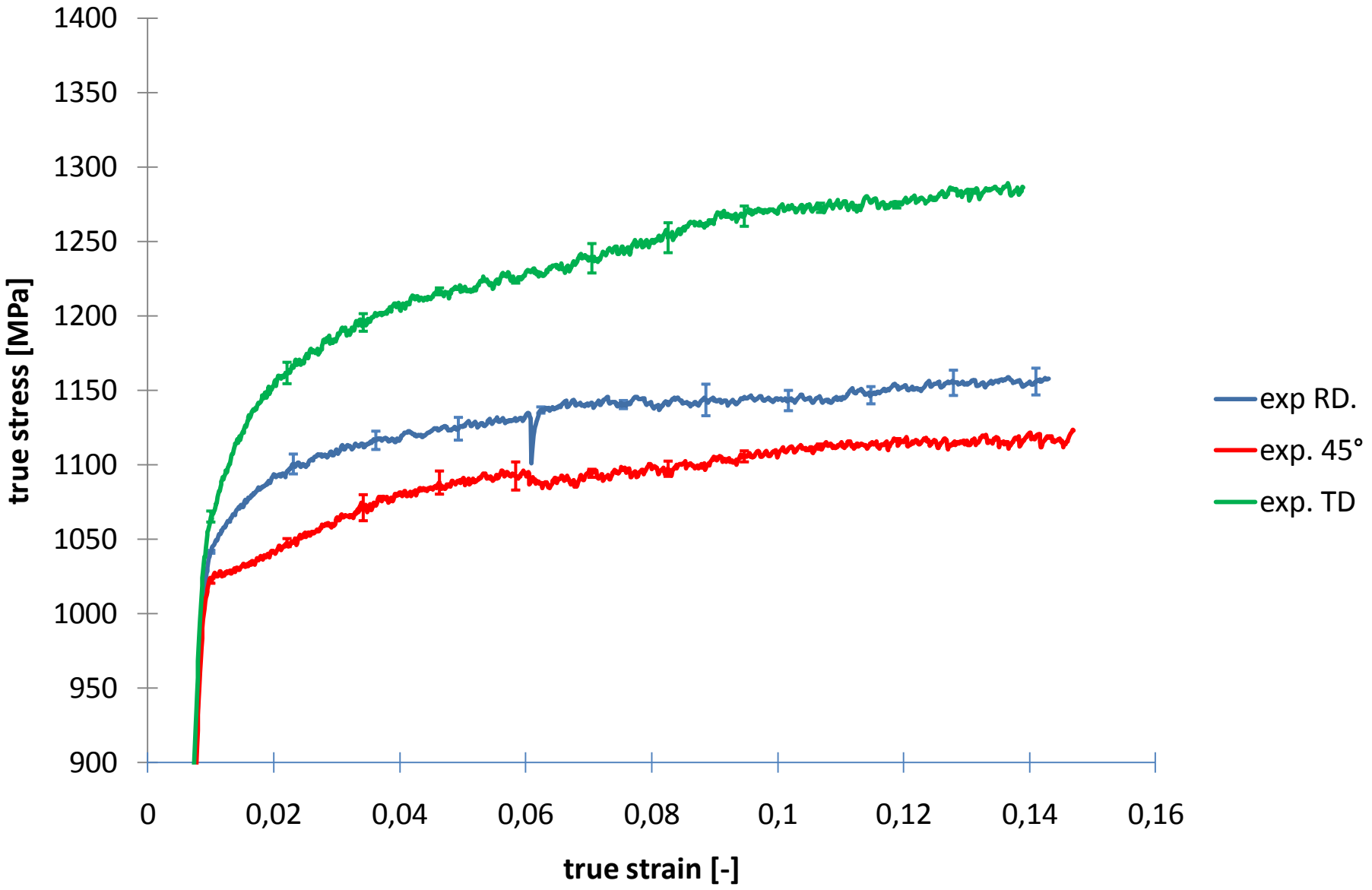

Twinning in our TA6V sheet ?

Small amount of measured twins (max 2,5 %)

All the hardening curves showing no or low increase of strain hardening

→Crystal plasticity model only based on slip system activation

→No twinning taken into account

Available Crystal Plasticity models

Van Houtte P, Li S, Seefeldt M, Delannay L. *Deformation texture prediction: from the Taylor model to the advanced Lamel model.* *IJP* (2005) ;21

Delannay L, Logé RE, Signorelli JW, Chastel Y. *Evaluation of a multisite model for the prediction of rolling textures in hcp metals.* *IJFP* 2005;8

- **Full Constraints (FC) Taylor's model**

$$\underline{\underline{L}}^{micro} = \underline{\underline{L}}^{macro}$$ Velocity gradient $\left(\underline{\underline{L}} = \frac{\partial \dot{\underline{u}}}{\partial \underline{x}} \right)$

$$\underline{\underline{\sigma}}^{macro} = \frac{1}{V} \int_{RVE} \underline{\underline{\sigma}}^{micro} dV$$ Cauchy stress

Stress equilibrium between adjacent grains not enforced

Crystal plasticity models

- **Relaxed Constraints (RC)** Taylor's model

$$\underline{\underline{L}}^{micro} = \underline{\underline{L}}^{macro}$$

Some components are relaxed (replaced by equilibrium conditions)

RC models for rolling:

➔ Lath model

RD-ND component relaxed

RD = Rolling Direction
TD = Transverse Direction
ND = Normal Direction

➔ Pancake model

RD-ND and TD-ND components relaxed

Crystal plasticity models

- **Multiple point models** **Groups of several grains are considered**

➔ **LAMEL** model for rolling

Groups of 2 grains with interface parallel to sheet plane

FC Taylor's condition applied to the group

RD-ND and TD-ND components relaxed

Compatibility and equilibrium fulfilled in the group

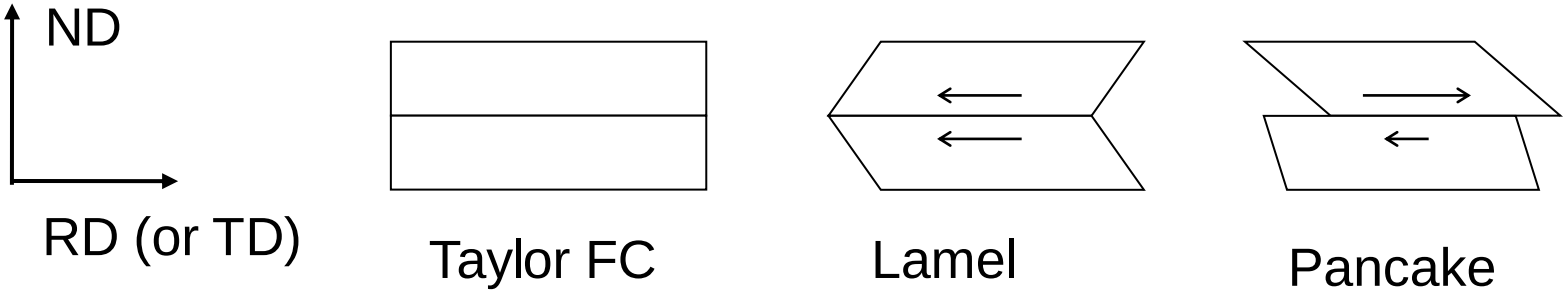

Crystal plasticity models

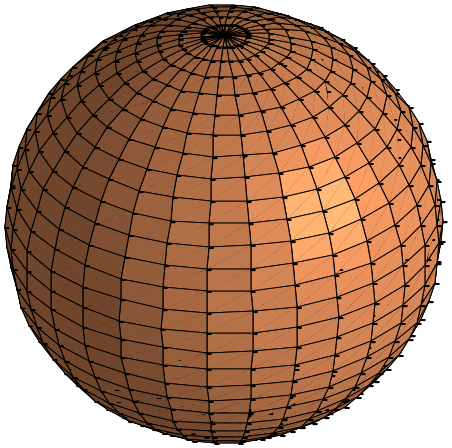

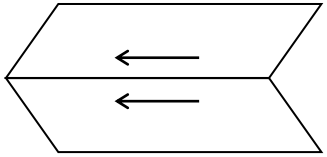

Adapted to any deformation process

ALAMEL model

Interface not anymore parallel to sheet plane

- spherical grains ➔ random orientation of the interfaces

Crystal plasticity models

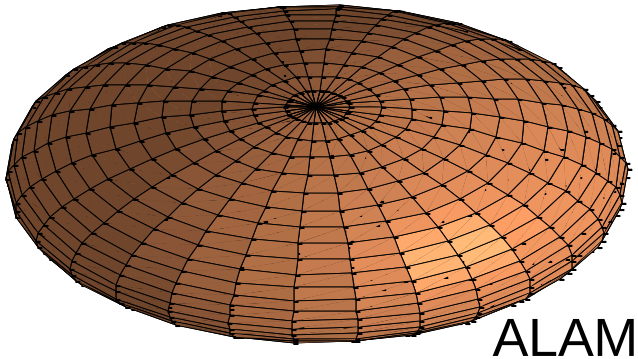

ALAMEL model

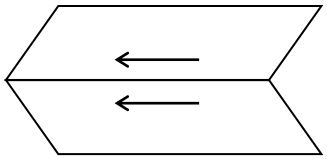

Adapted to any deformation process

Interface not anymore parallel to sheet plane

Examples: - spherical grains ➔ random orientation of the interfaces

- flat grains ➔ preferred orientation parallel to grain plane

Crystal plasticity models

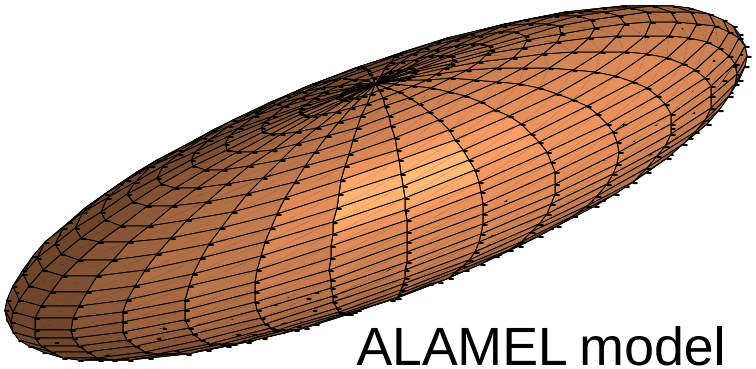

ALAMEL model

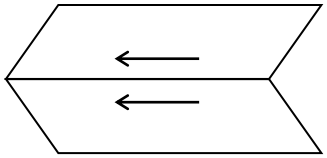

Adapted to any deformation process

Interface not anymore parallel to sheet plane

Examples: - spherical grains ➔ random orientation of the interfaces

- flat grains ➔ preferred orientation parallel to grain plane

- elongated grains (needle) ➔ preferred orientations of the interface containing the grain axis

Crystal plasticity models

Flow rule

$$\dot{\gamma}_\alpha = \dot{\gamma}_0 \left| \frac{\tau^\alpha}{\tau_{CRSS}} \right|^{\frac{1}{m}} sign(\tau^\alpha)$$

Hardening

$$\tau_{CRSS} = \tau_{C0} \left(1 + \frac{\Gamma_{tot}}{\Gamma_0} \right)^n$$

with $\Gamma_{tot} = \int_0^t \sum_\alpha \left| \dot{\gamma}_\alpha \right| dt$

$\dot{\gamma}_\alpha$ Slip rate on slip system α

τ^α Shear stress on slip system α

τ_{CRSS} Critical Resolved Shear Stress

Γ_{tot} **Accumulated plastic slip**

No specific hardening per family

Low number of parameters

Material parameters:

$\dot{\gamma}_0$ $1/m$ τ_{C0} Γ_0 n

Strain rate sensitivity

Identification of Crystal Plasticity Models on Tensile tests

constant strain rate : $3 \times 10^{-4}\ s^{-1}$

Strain field measured by DIC → Lankford coeff $r \equiv \frac{\dot{\varepsilon}_w^p}{\dot{\varepsilon}_t^p} = -\frac{\dot{\varepsilon}_w^p}{\dot{\varepsilon}_l^p + \dot{\varepsilon}_w^p}$

→ True stress – True strain curves

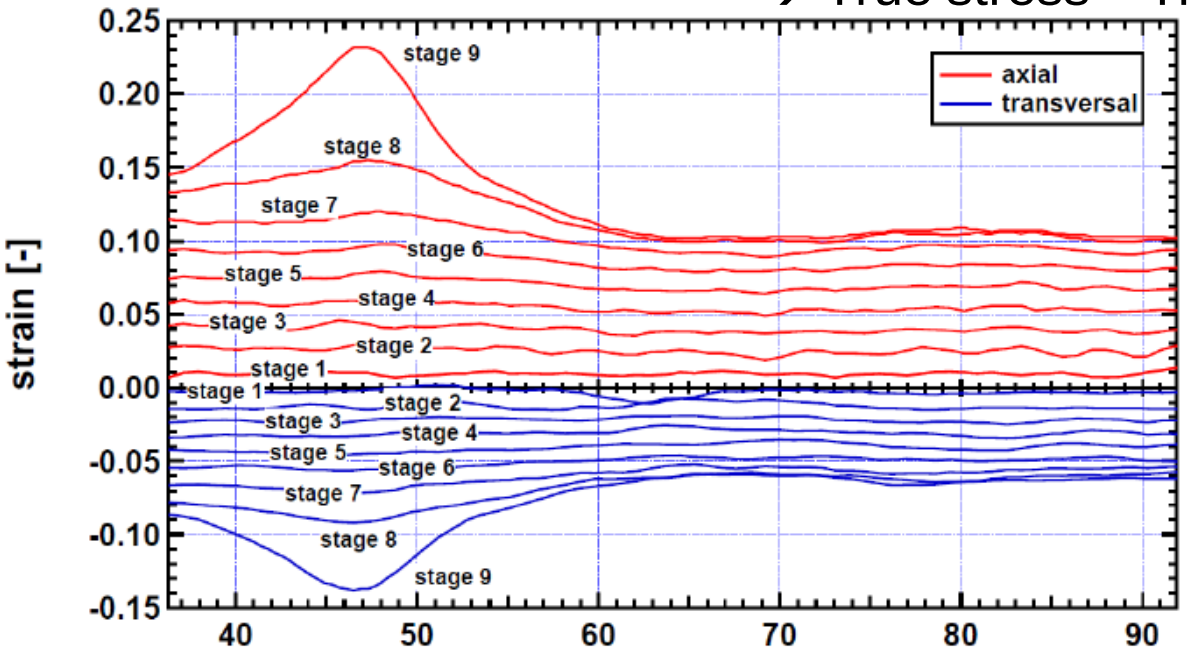

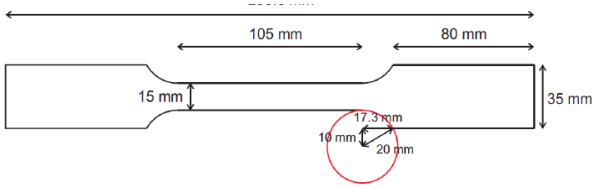

Strain rate effect
Room temperature. Static tests

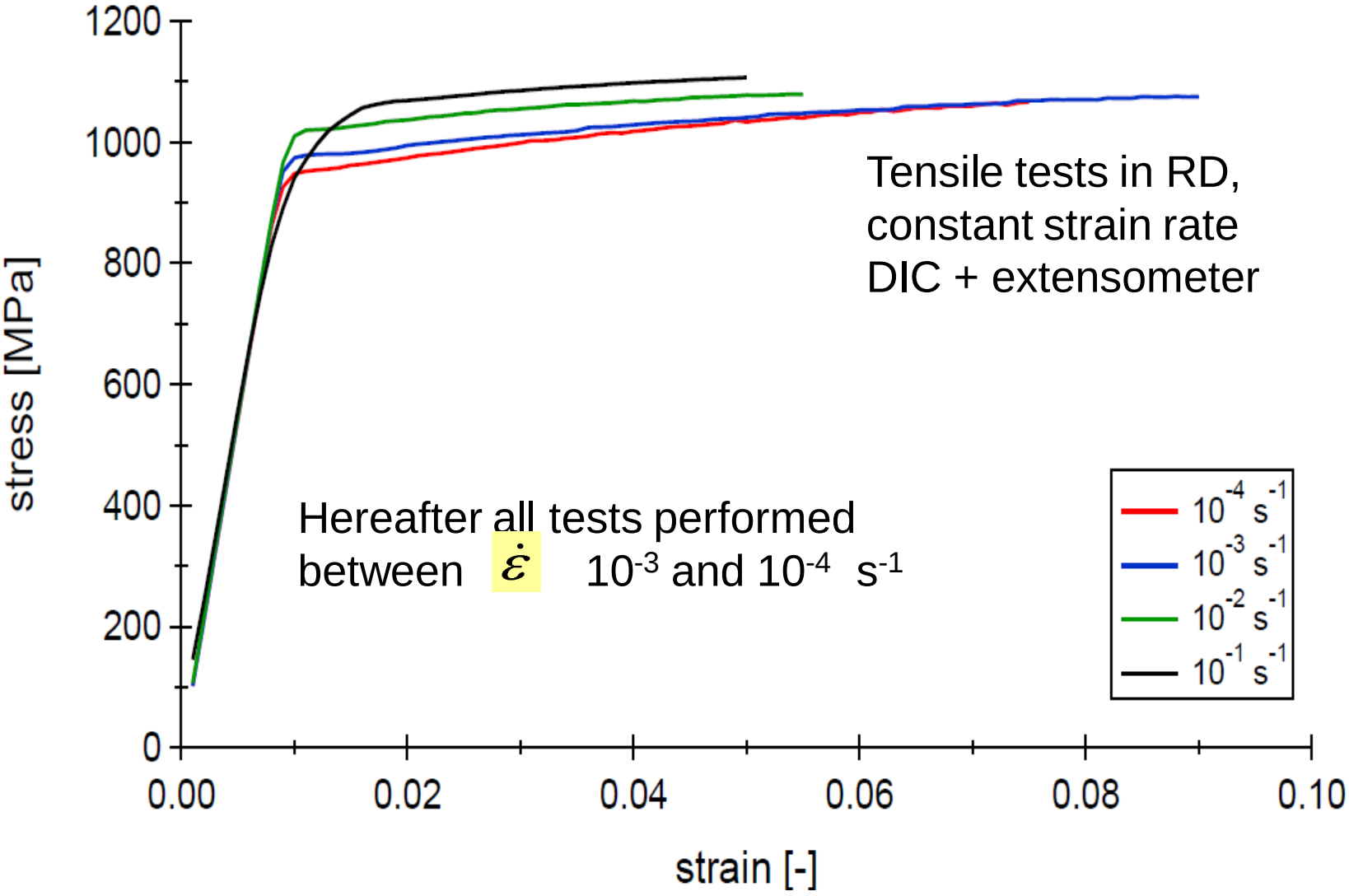

Constant strain rate tensile tests in Ulg lab

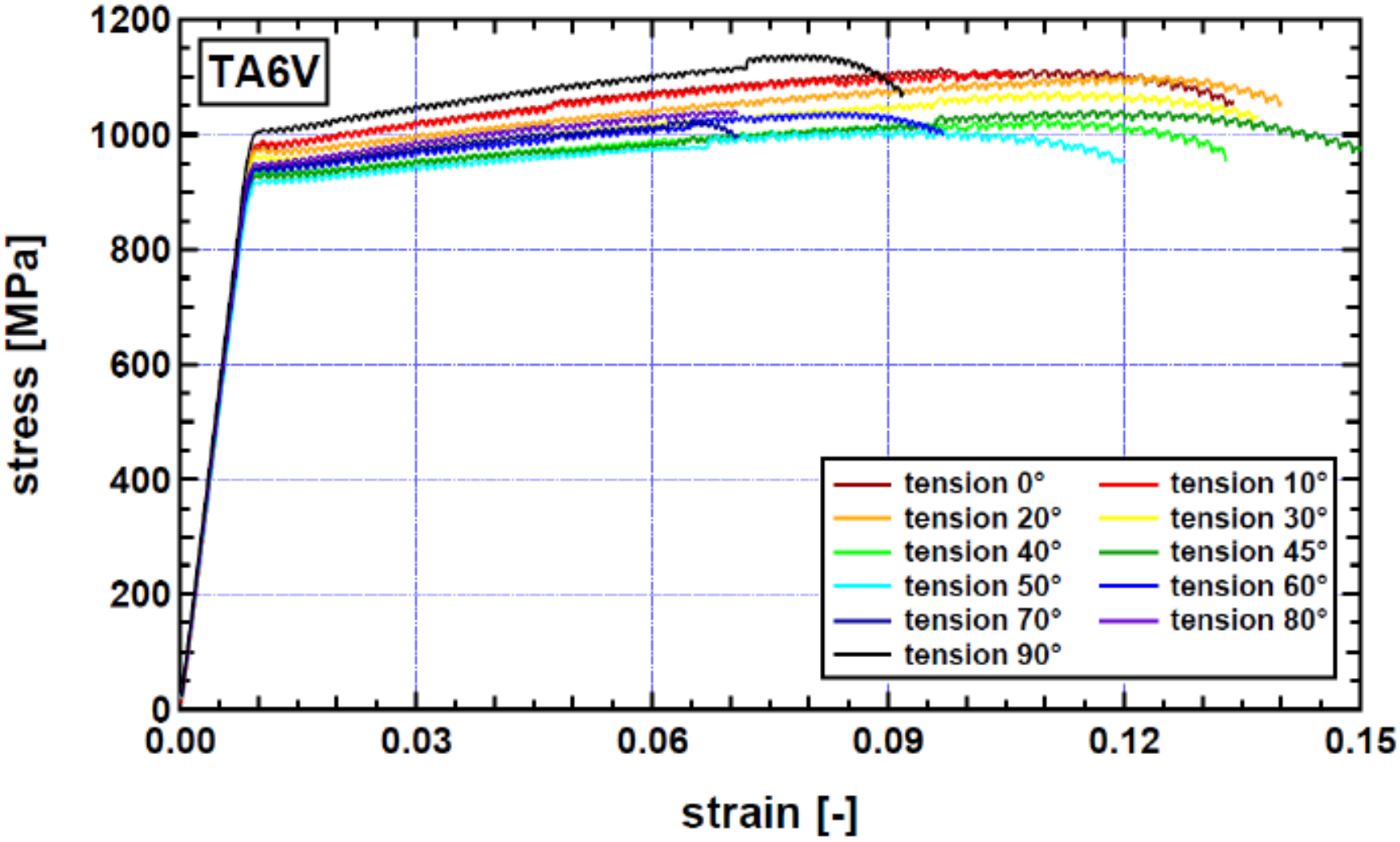

Identification of Crystal Plasticity Models

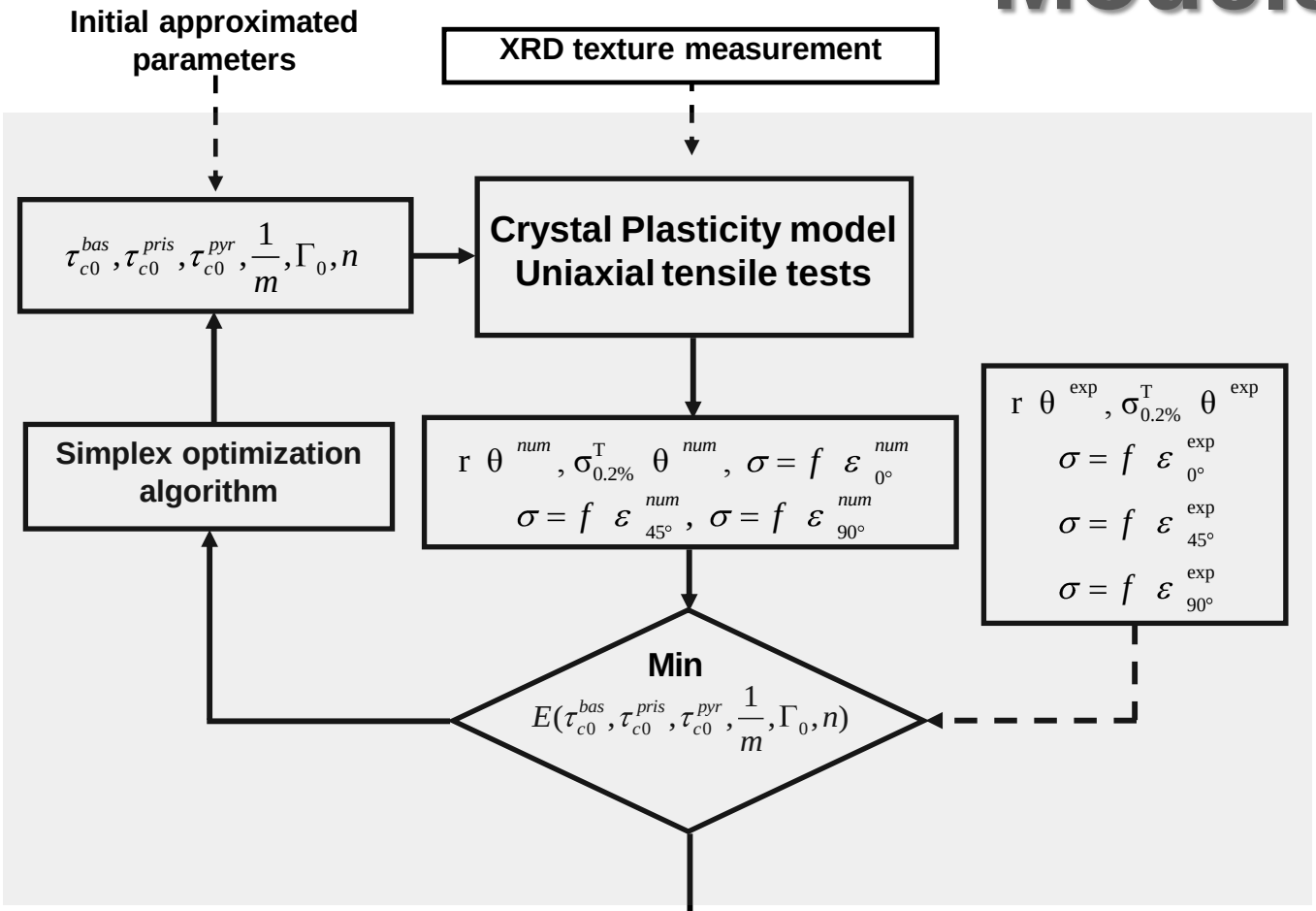

$$\theta = 0, 10, 20, \ldots, 90$$

Crystal Plasticity Models

Initial texture defined by a set of 3000 orientations

BCC β phase with a single CRSS of 300 Mpa (Gerday *Acta Mat (* 2009) 57)

Error function : sum of distance between predictions and tests:

$$E_r = \sqrt{\frac{1}{n}\sum_{j=1}^{n}\left(\frac{r(\theta)^{\exp} - r(\theta)n^{um}}{r(\mathbf{0})^{\exp}}\right)^2}$$

n= 11 directions

Same impact of all the experimental results

$$r\ \theta^{\exp},\ \sigma^{T}_{0.2\%}\ \theta^{\exp}$$

$$\sigma = f\ \varepsilon^{\exp}_{0°}$$

$$\sigma = f\ \varepsilon^{\exp}_{45°}$$

$$\sigma = f\ \varepsilon^{\exp}_{90°}$$

Predictions of Planar Anisotropy

Lankford coefficient for tensile tests in different directions

Constant values with strain

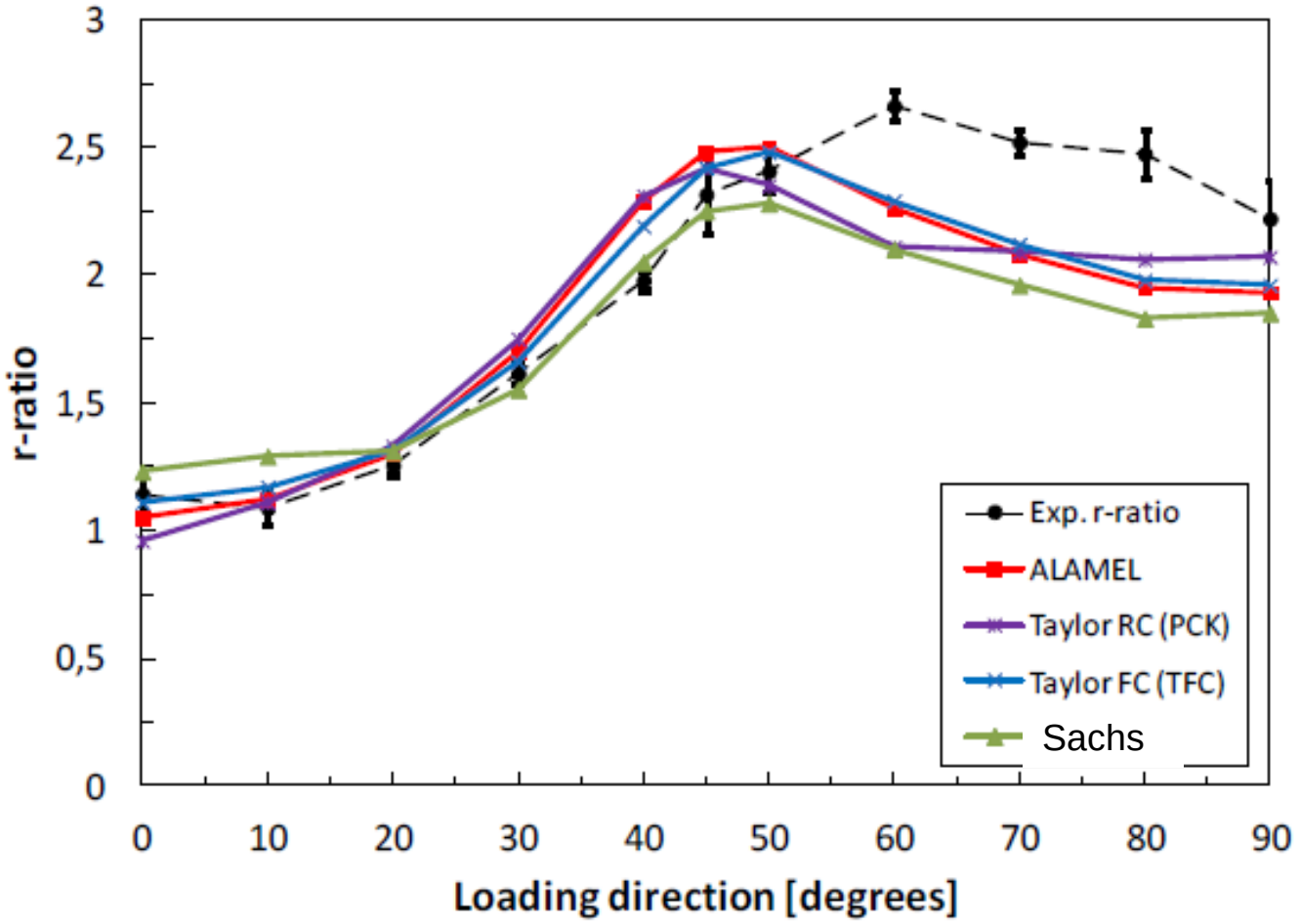

Predictions with the optimal set of CRSS minimizing the error for each model

Alamel or Taylor FC ???

Predictions of Planar Anisotropy

Yield stresses in tensile in different directions

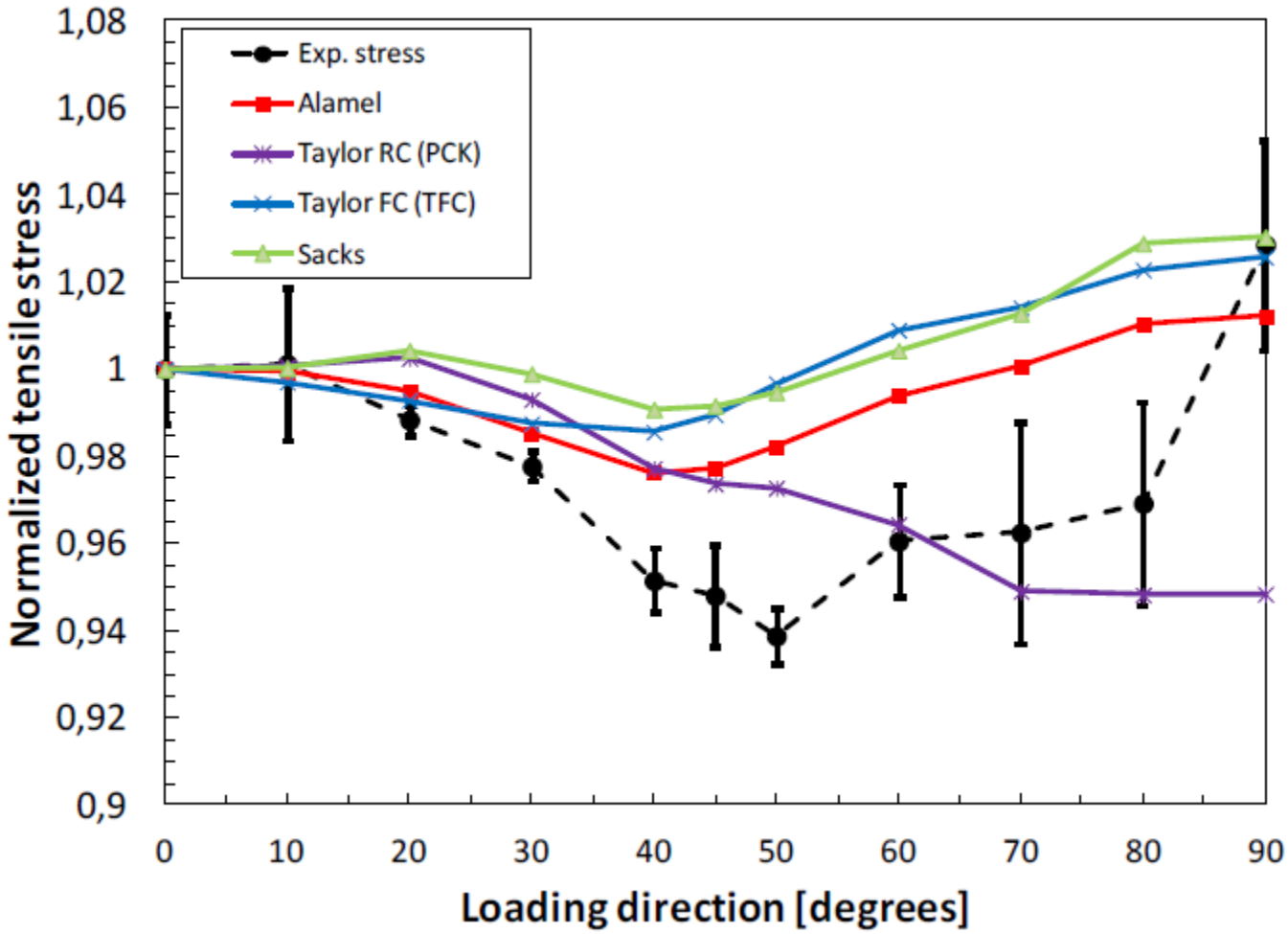

Predictions with the optimal set of CRSS minimizing the error for each model

Alamel ~~or Taylor FC ???~~ = chosen model

Identified CRSS

(MPa)	τ_{prism}	τ_{basal}	τ_{pyram}	$\tau_{basal}/\tau_{prism}$	$\tau_{pyram}/\tau_{prism}$
Taylor FC	449	337,5	656	0.75	1.46
Taylor RC (PCK)	484	394	573	0.81	1.18
Sachs	501	421	922	0.84	1.84
Alamel	**442**	**349**	**701**	**0.79**	**1.59**
CPFEM (Dick)				*1.05*	*1.6*
Sachs (Perilla, Gil Sevillano) sheet				*0.93 – 1.3*	*1.1 -1.6*

1/m = 25 n=0.9 $\Gamma_0 = 2$

Orthotropic yield criterion CPB06exn

Cazacu et al. (2006), Orthotropic yield criterion for hcp metals, **IJP**, 22, p.p. 1171-1194

Plunkett et al. (2008), Orthotropic yield criteria for description of the anisotropy in tension and compression of sheet metals**, IJP** 24, p.p. 847-866

Plunkett et al. (2006), Anisotropic yield function of hexagonal materials taking into account texture development and anisotropic hardening, **Acta Mat,** 54, p.p. 4159-4169

Gilles et al (2011) Experimental characterization and elasto-plastic modeling of the quasi-static mechanical response of TA-6 V at room temperature, **IJSS** 48(9),

Gilles et al (2012) Experimental and numerical study of TA-6V mechanical behavior in different monotonic loading conditions at room temperature, **Procedia IUTAM (2012), 3**

Orthotropic yield criterion CPB06exn

n linear transformations: $\boldsymbol{\Sigma}^1 = \mathbf{C}^1 : \mathbf{S}, \boldsymbol{\Sigma}^2 = \mathbf{C}^2 : \mathbf{S}, \ldots, \boldsymbol{\Sigma}^n = \mathbf{C}^n : \mathbf{S}$

S: deviator of Cauchy's stress tensor

$$\mathbf{C}^i = \begin{pmatrix} C_{11}^i & C_{12}^i & C_{13}^i & 0 & 0 & 0 \\ C_{12}^i & C_{22}^i & C_{23}^i & 0 & 0 & 0 \\ C_{13}^i & C_{23}^i & C_{33}^i & 0 & 0 & 0 \\ 0 & 0 & 0 & C_{44}^i & 0 & 0 \\ 0 & 0 & 0 & 0 & C_{55}^i & 0 \\ 0 & 0 & 0 & 0 & 0 & C_{66}^i \end{pmatrix}$$

anisotropy coefficients

$$F = \sum_{i=1}^{n} \left[\left| \Sigma_1^{(i)} \right| - k^{(i)} \Sigma_1^{(i)} \right]^a + \left| \Sigma_2^{(i)} \right| - k^{(i)} \Sigma_2^{(i)} \Big]^a + \left| \Sigma_3^{(i)} \right| - k^{(i)} \Sigma_3^{(i)} \Big]^a$$

$\Sigma_1^i, \Sigma_2^i, \Sigma_3^i$: eigenvalues of $\boldsymbol{\Sigma}^i$

$a \geq 1$ (integer) : degree of homogeneity

$-1 \leq k^i \leq 1$: SD parameters

k strength differential parameter

Identification of CPB06exn shape

Parameter optimization technique: simulated annealing method

Metropolis *et al. (1953); Hastings (1970)*

Tensile yield stress

Lankford coeff (tensile)

Compression yield stress

$$E = \sum_i \frac{\omega_i}{\Omega}\left[\frac{\sigma_\theta^T / \sigma_0^T \;{}^{\text{th}}_{i}}{\sigma_\theta^T / \sigma_0^T \;{}^{\text{exp}}_{i}} - 1\right]^2 + \sum_j \frac{\omega_j}{\Omega}\left[\frac{r_\theta^T \;{}^{\text{th}}_{j}}{r_\theta^T \;{}^{\text{exp}}_{j}} - 1\right]^2 + \sum_k \frac{\omega_k}{\Omega}\left[\frac{\sigma_\theta^C / \sigma_0^T \;{}^{\text{th}}_{k}}{\sigma_\theta^C / \sigma_0^T \;{}^{\text{exp}}_{k}} - 1\right]^2$$

$$+ \sum_l \frac{\omega_l}{\Omega}\left[r_\theta^{PS} \;{}^{\text{th}}_{l}\right]^2 + \sum_m \frac{\omega_m}{\Omega}\left[\frac{\sigma_\theta^{SSH} / \sigma_0^T \;{}^{\text{th}}_{m}}{\sigma_\theta^{SSH} / \sigma_0^T \;{}^{\text{exp}}_{m}} - 1\right]^2$$

Plane strain condition should be 0

Shear yield stress

$$\Omega = \sum_i \omega_i + \sum_j \omega_j + \sum_k \omega_k + \sum_l \omega_l + \sum_m \omega_m$$

Plane strain results

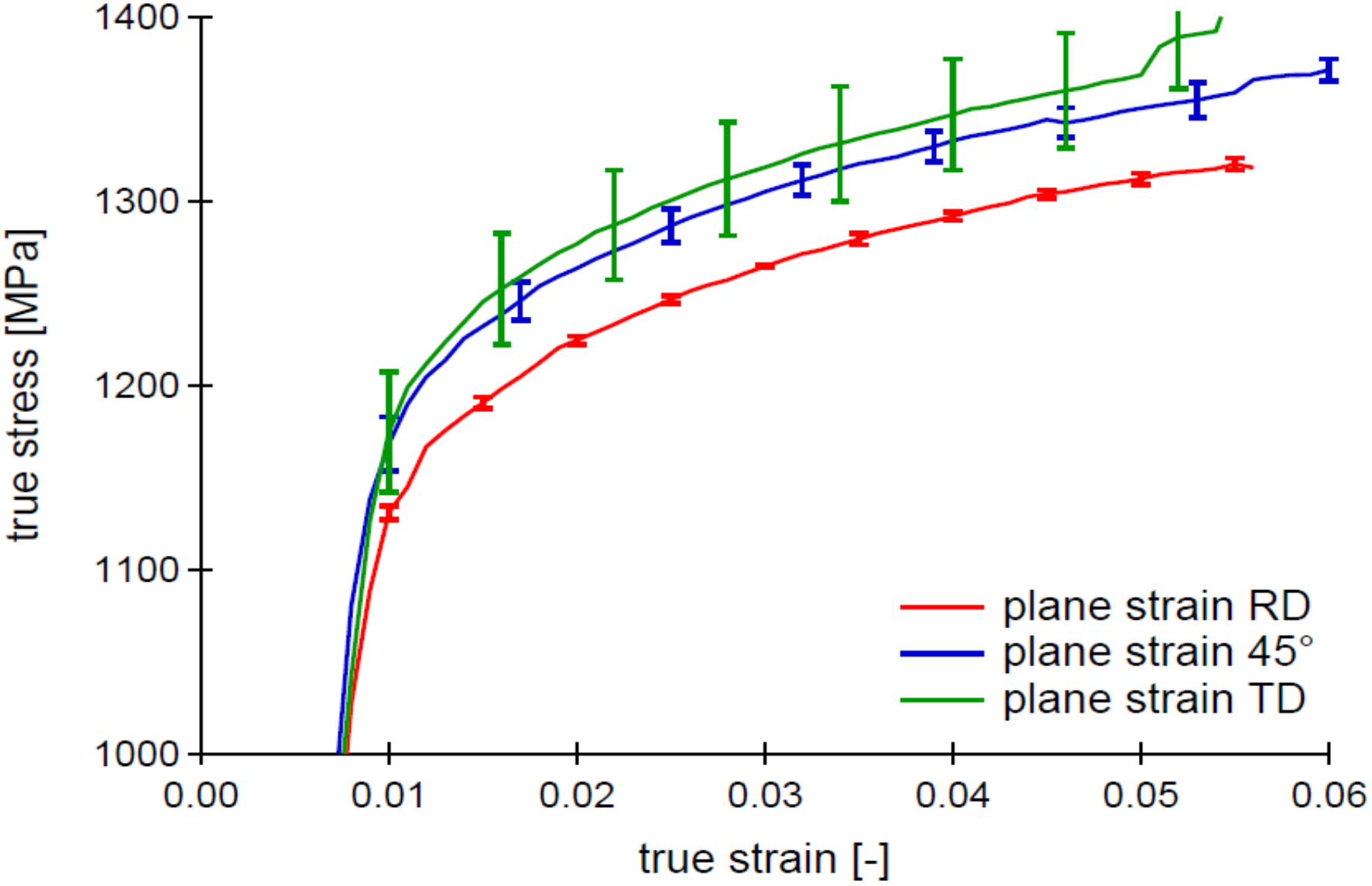

Identification of CPB06exn Shape

IJSS (a= 2, C_{11} =C'$_{11}$ =C''$_{11}$ =1 C_{44}=C_{55}=C_{66}…')
3 linear transformations
Tensile tests in 0, 10, … 80, 90 from RD: yield stresses + Lankford coeff.
Compression tests in 0 45 and 90 from RD: yield stress

IUTAM (a= 2, C_{11} =1 C_{44}=C_{55}=C_{66} (simplified IJSS)
1 linear transformation
Tensile tests in 0, 45 , 90 from RD: yield stresses + Lankford coeff.
Compression tests in 0 45 and 90 from RD: yield stress

New a2 (a free found = 2, C_{11} =1 C_{44}=C_{55}=C_{66}) (all tests)
1 linear transformation
Tensile tests in 0, 10, … 80, 90 from RD: yield stresses + Lankford coeff.
Compression tests in 0 45 and 90 from RD: yield stress
Plane strain tests in 0 45 and 90 from RD:: yield stress
Simple shear 0 45 and 90 from RD:: yield stress

New a4 (a = 4, C_{11} =1 C_{44}=C_{55}=C_{66}) (a=4 imposed)

About hardening in Cazacu model

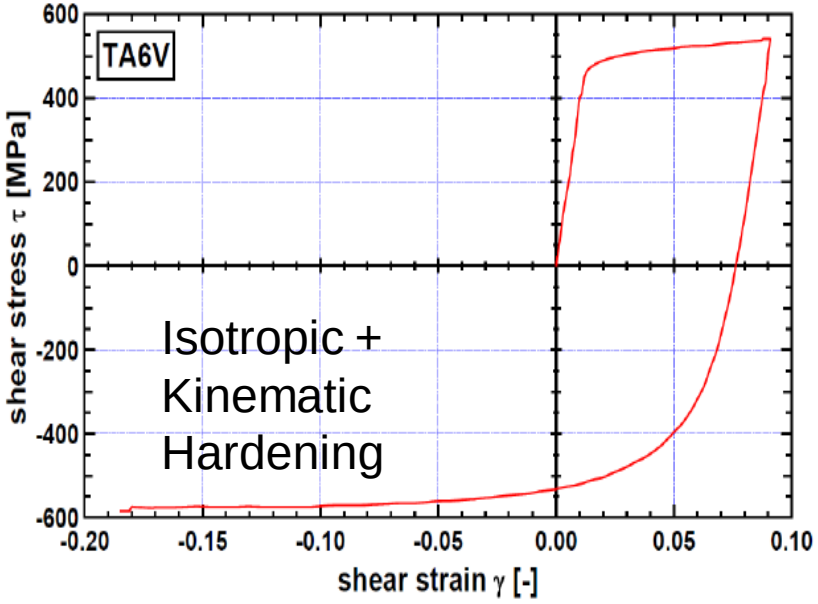

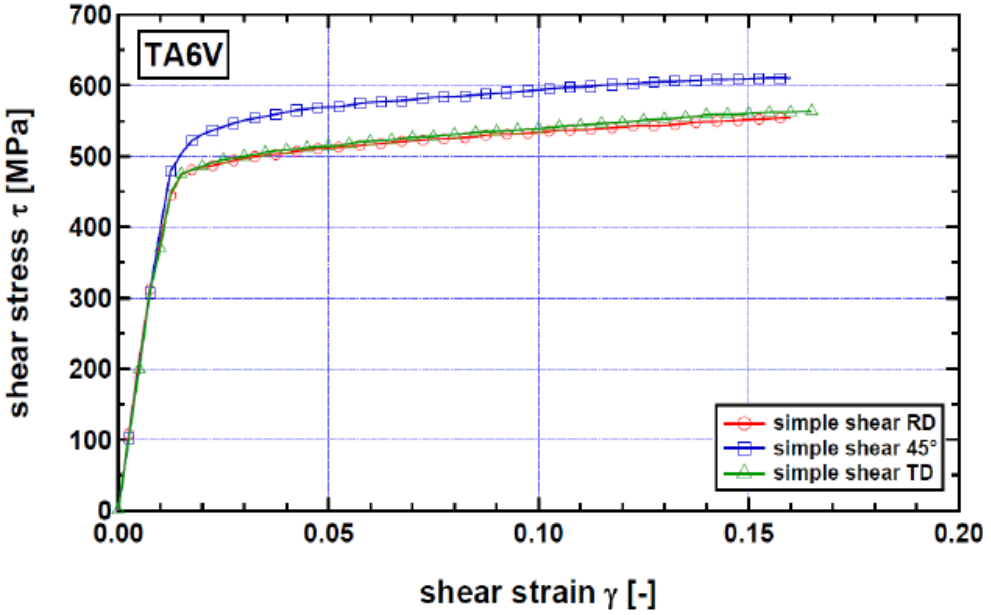

Simplification:

-only isotropic hardening of Voce identified on tensile in RD

$$Y\left(\overline{\varepsilon}^{p}\right) = R_0 + R \qquad dR = c_R\left(s_R - R\right)d\overline{\varepsilon}^{p}$$

(other approach: yield locus identified at 3 levels of plastic work + interpolation)

Identification results of CPB06exn

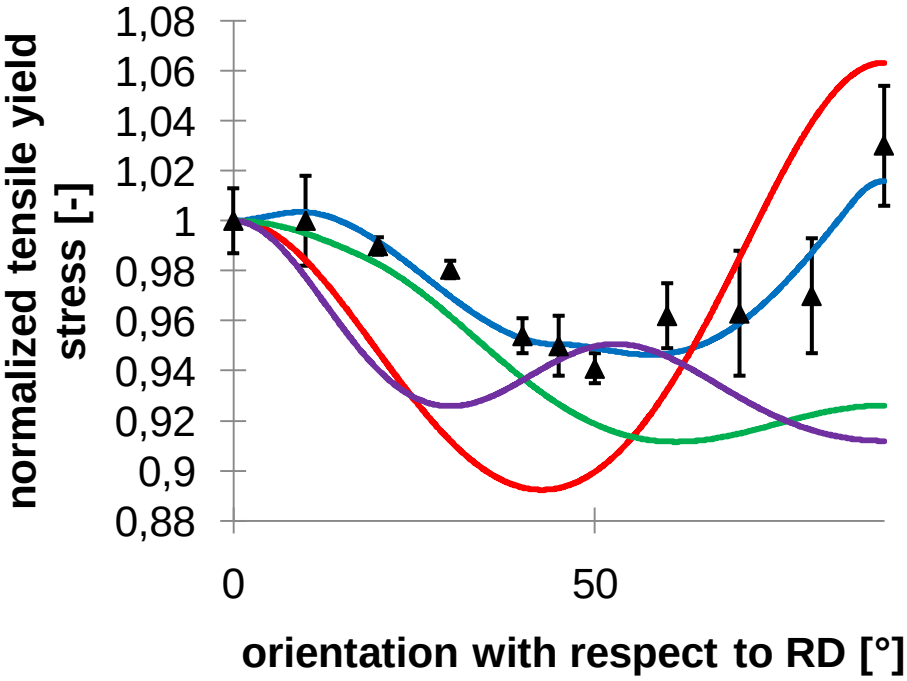

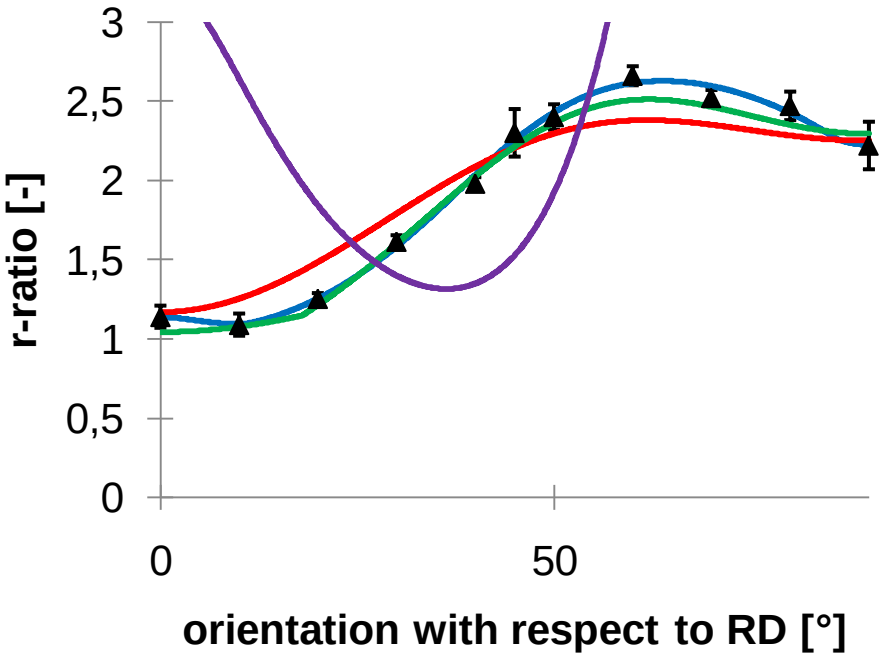

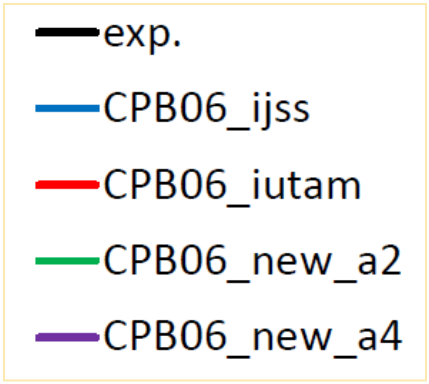

Without surprises IJSS = winner

Identification in IJSS is mainly focused on these tests

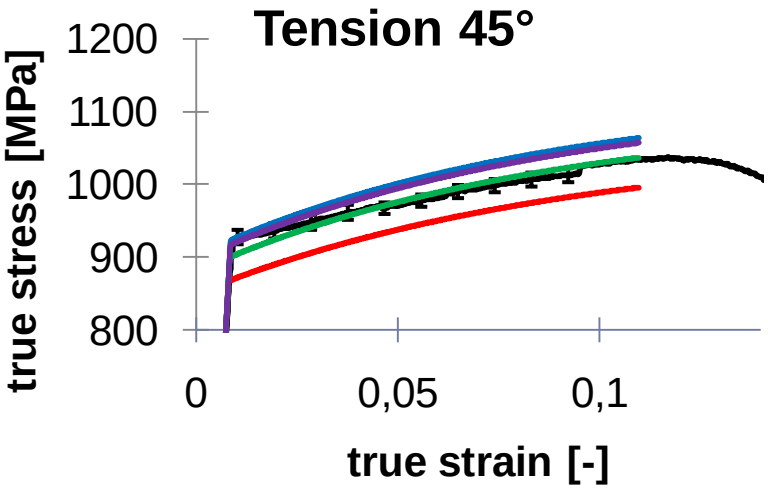

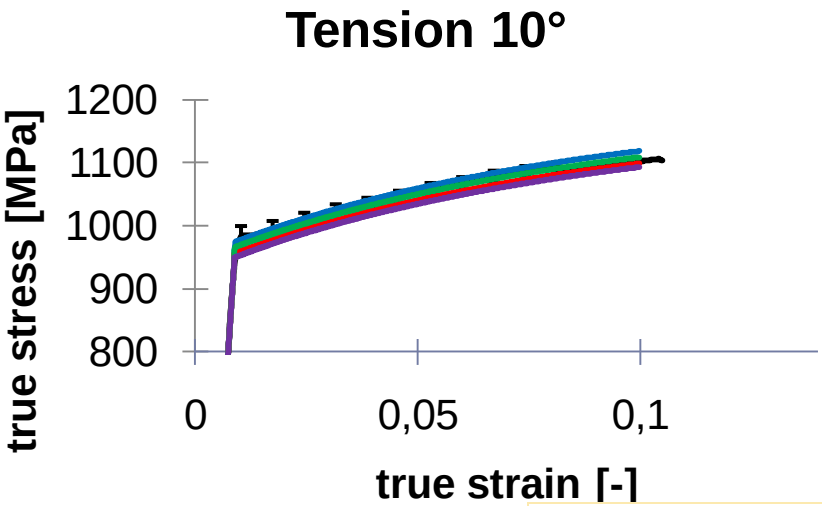

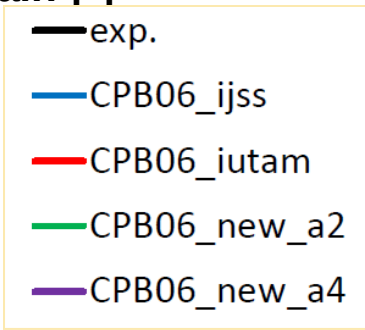

Clear winner **IJSS** looking at all directions

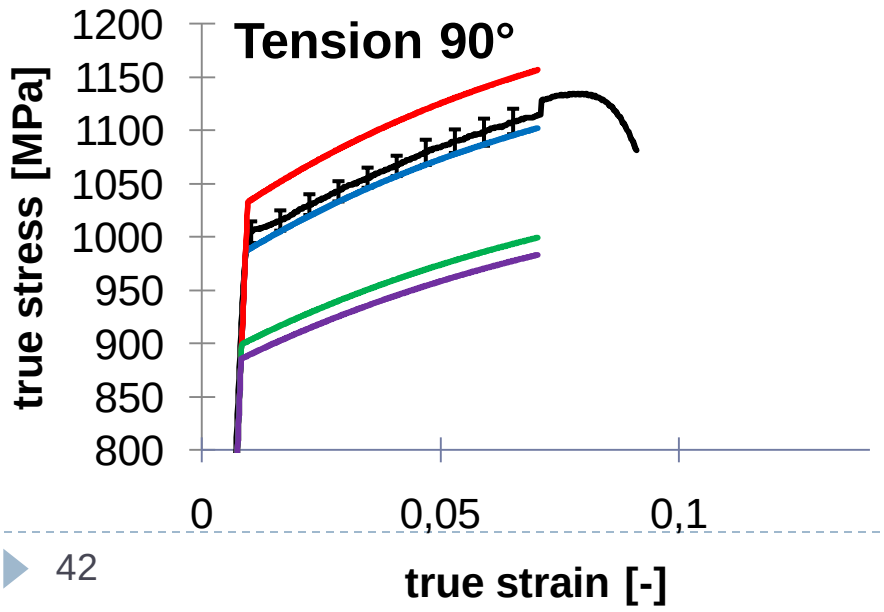

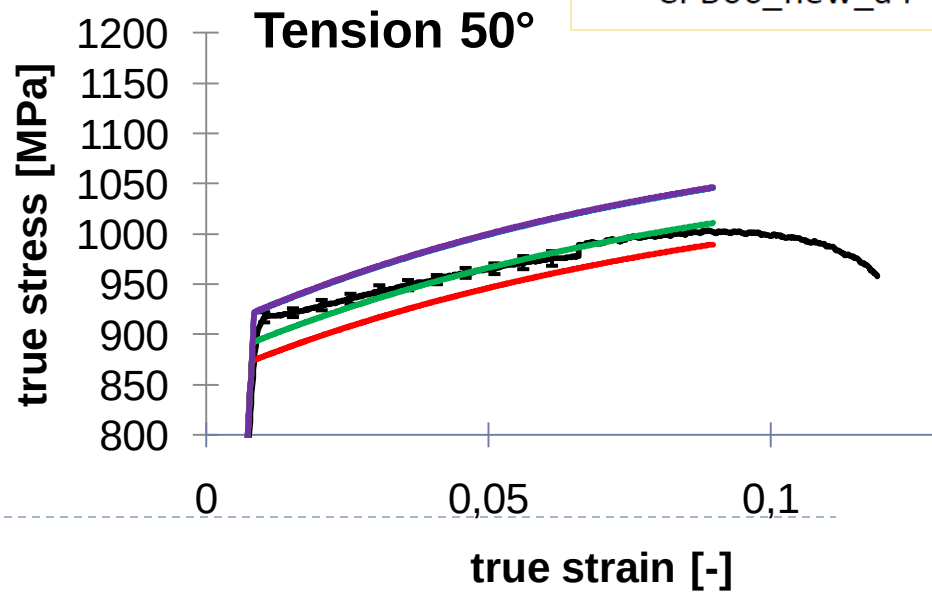

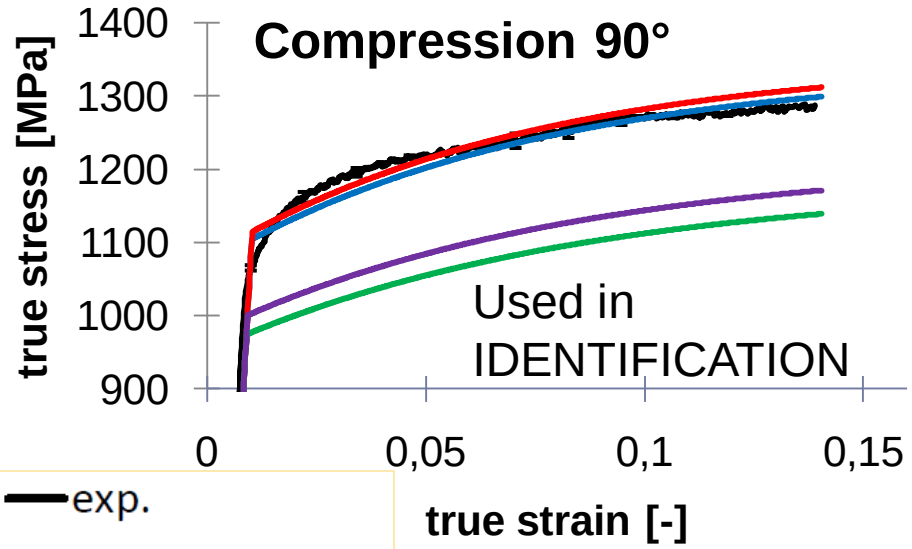

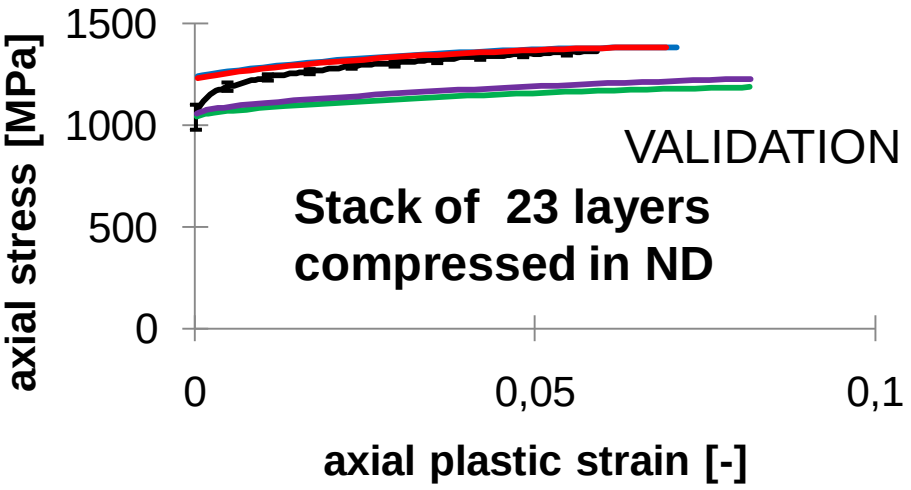

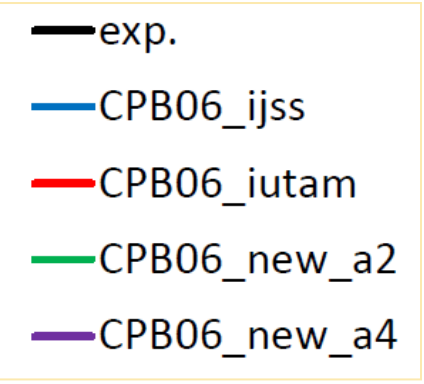

The winner is **IJSS** or **IUTAM** ?

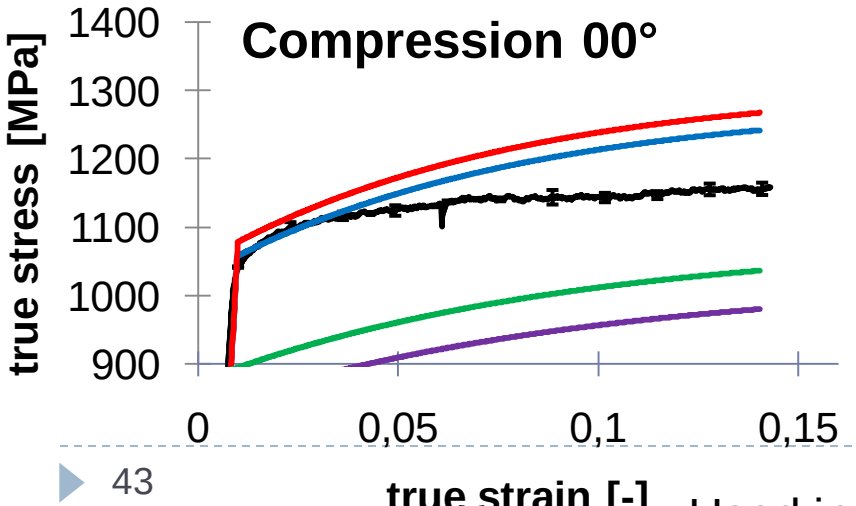

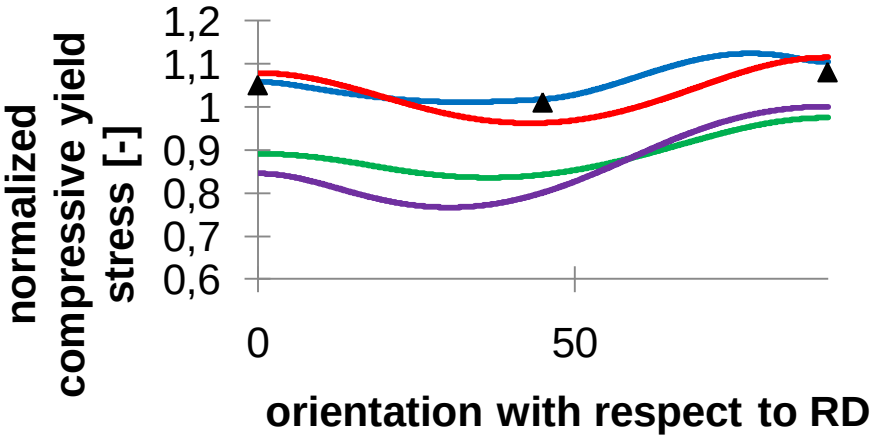

Used in IDENTIFICATION

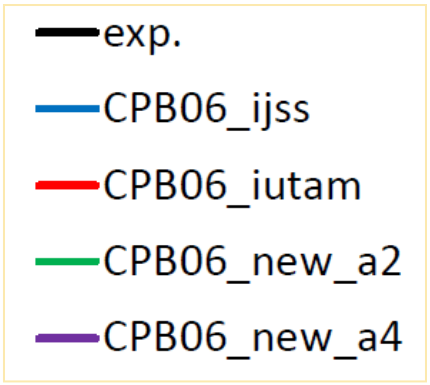

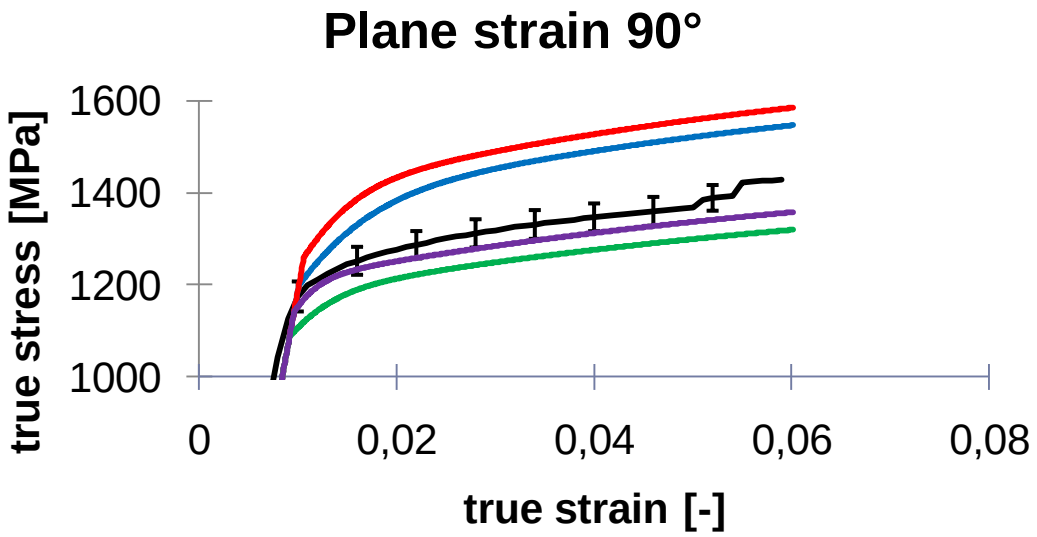

The winner is ??? **new a2** or IJSS = IUTAM?

Tests included in identification

Prediction, validation

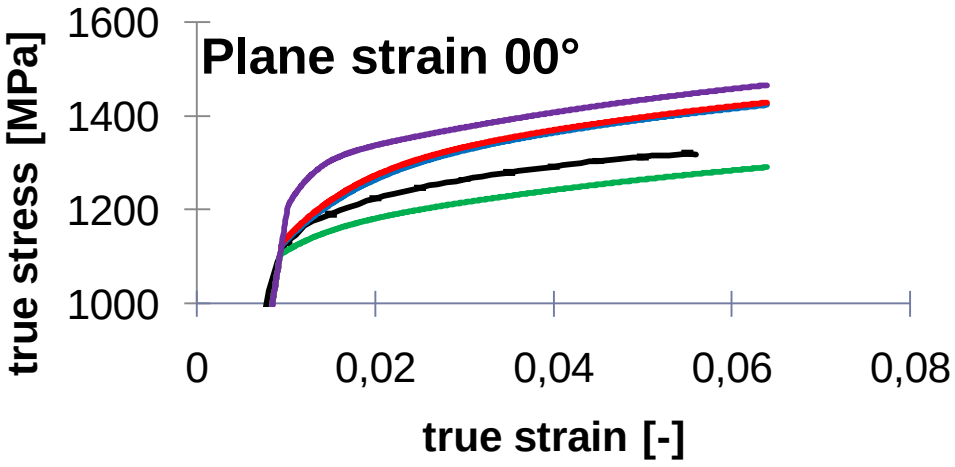

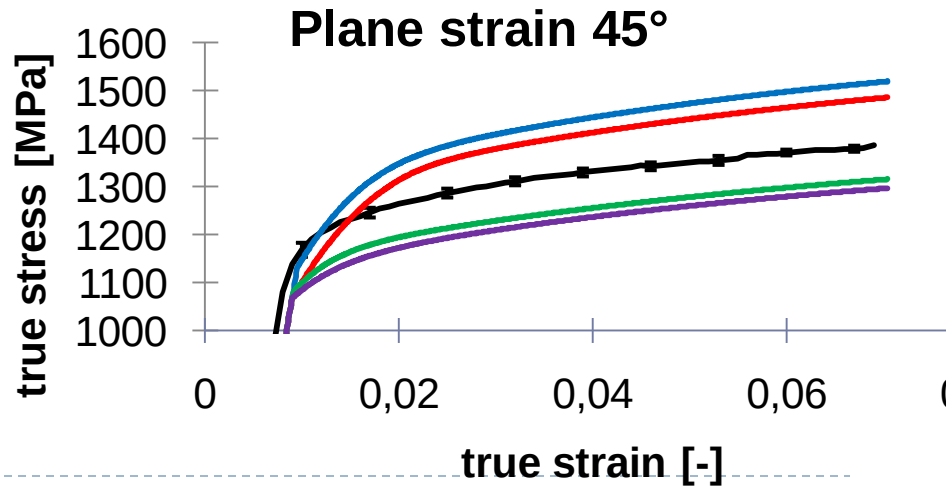

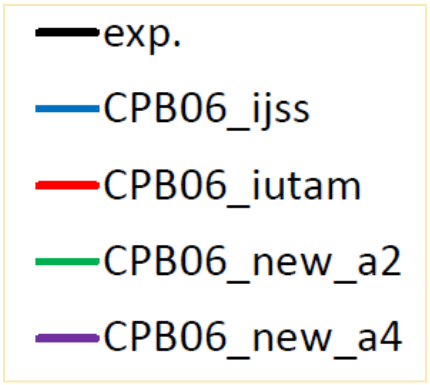

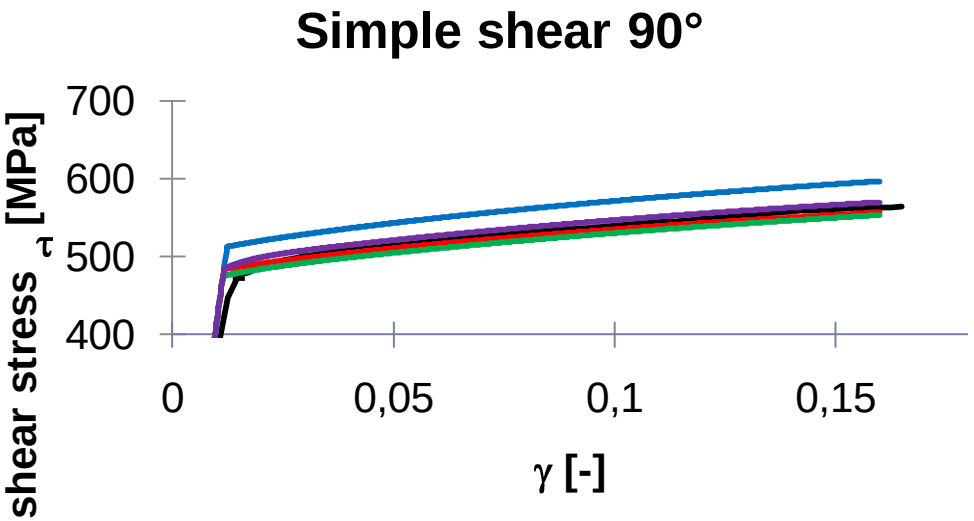

The winner is ??? **new a4** or **new a2** or **IUATAM** **IJSS** **??**

Tests included in identification Prediction, validation

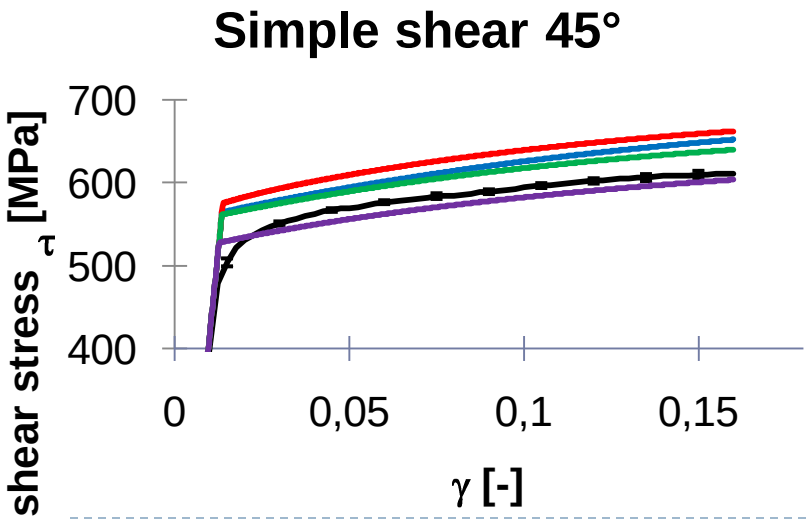

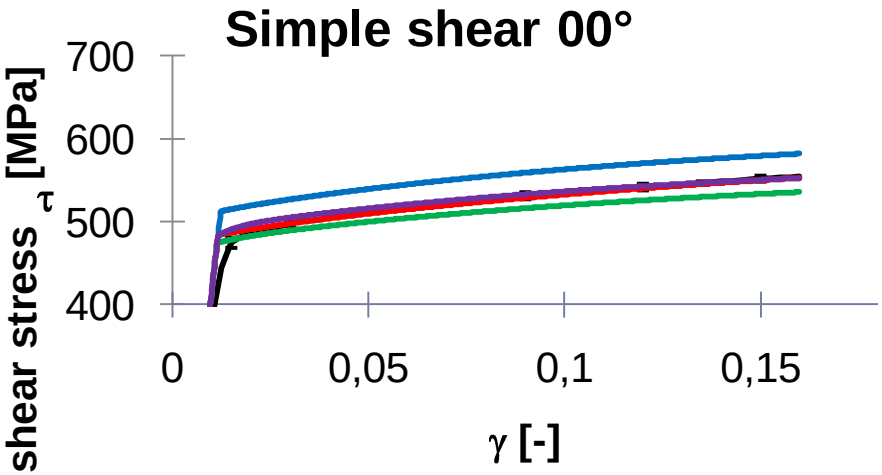

Predicted Yield loci

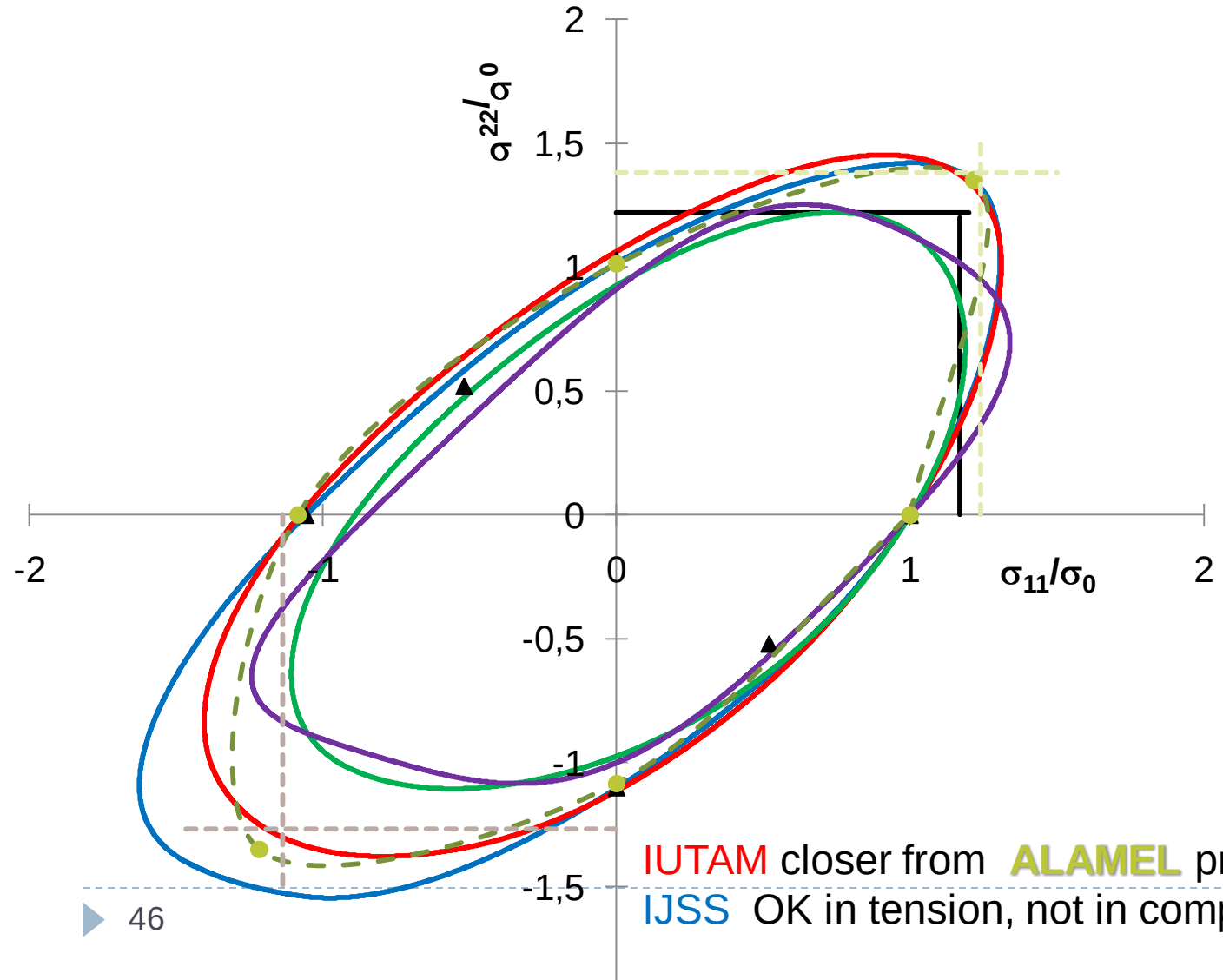

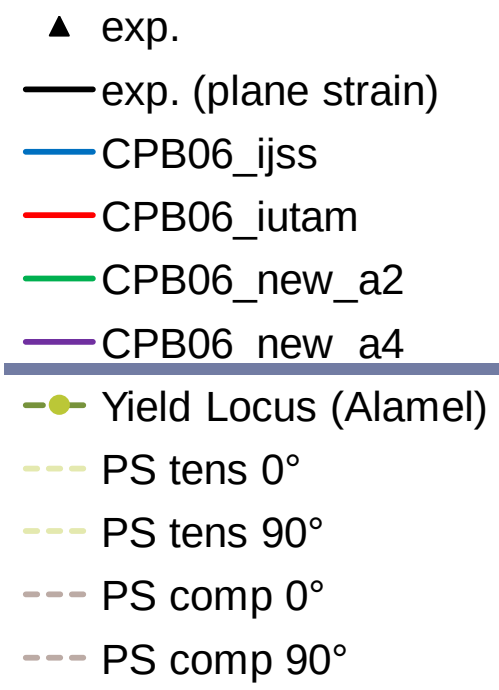

IUTAM closer from ALAMEL prediction

IJSS OK in tension, not in compression, with ALAMEL

Comparison Cazacu // Lamel // Experiments

Compression

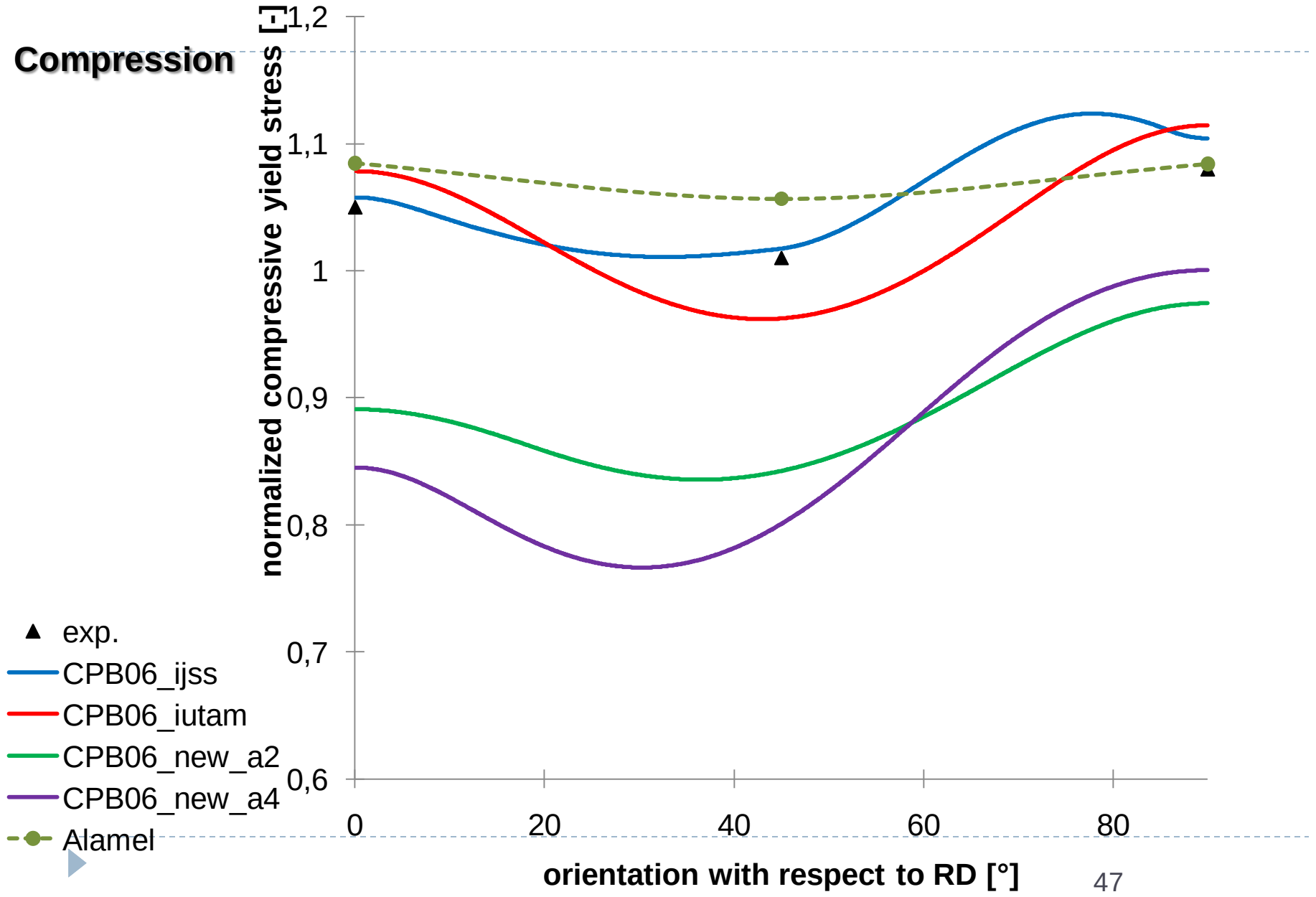

Error estimation

	CPB06_ijss	CPB06_iutam	CPB06_new_a2	CPB06_new_a4	ALAMEL
$\sum_i \left[\frac{\sigma_\theta^T / \sigma_0^T{}_i^{\text{th}}}{\sigma_\theta^T / \sigma_0^T{}_i^{\text{exp}}} - 1 \right]^2$	9.2 x 10^{-4}	2.36 x 10^{-2}	1.91 x 10^{-2}	2.39 x 10^{-2}	8.75 x 10^{-3}
$\sum_j \left[\frac{r_\theta^T{}_j^{\text{th}}}{r_\theta^T{}_j^{\text{exp}}} - 1 \right]^2$	3.13 x 10^{-3}	9.92 x 10^{-2}	1.77 x 10^{-2}	37.56	0.16
$\sum_k \left[\frac{\sigma_\theta^C / \sigma_0^T{}_k^{\text{th}}}{\sigma_\theta^C / \sigma_0^T{}_k^{\text{exp}}} - 1 \right]^2$	2.56 x 10^{-5}	3.65 x 10^{-3}	6.88 x 10^{-2}	9.55 x 10^{-2}	2.03 x 10^{-3}
$\sum_l \left[\frac{\sigma_\theta^{PS} / \sigma_0^T{}_l^{\text{th}}}{\sigma_\theta^{PS} / \sigma_0^T{}_l^{\text{exp}}} - 1 \right]^2$	9.67 x 10^{-4}	1.12 x 10^{-2}	1.18 x 10^{-2}	1.27 x 10^{-2}	3.39 x 10^{-2}
$\sum_m \left[\frac{\sigma_\theta^{SSH} / \sigma_0^T{}_m^{\text{th}}}{\sigma_\theta^{SSH} / \sigma_0^T{}_m^{\text{exp}}} - 1 \right]^2$	1.35 x 10^{-2}	9.75 x 10^{-3}	3.83 x 10^{-3}	2.45 x 10^{-2}	4.67 x 10^{-2}
$\left[\frac{\sigma_\theta^{LCT} / \sigma_0^{T\,\text{th}}}{\sigma_\theta^{LCT} / \sigma_0^{T\,\text{exp}}} - 1 \right]^2$	8.84 x 10^{-3}	7.31 x 10^{-3}	5.92 x 10^{-3}	4.68 x 10^{-3}	7.31 x 10^{-5}
Error	0.0274	0.155	0.127	37.72	0.251

Final choice for Cazacu model

IJSS set of material parameters

Only model

→OK for yield points in tensile in all directions and in compression
→OK for Lankford points in all directions

However

→ Not too good in plane strain
→ Not good in shear curve

Comparison Cazacu // Lamel // Experiments

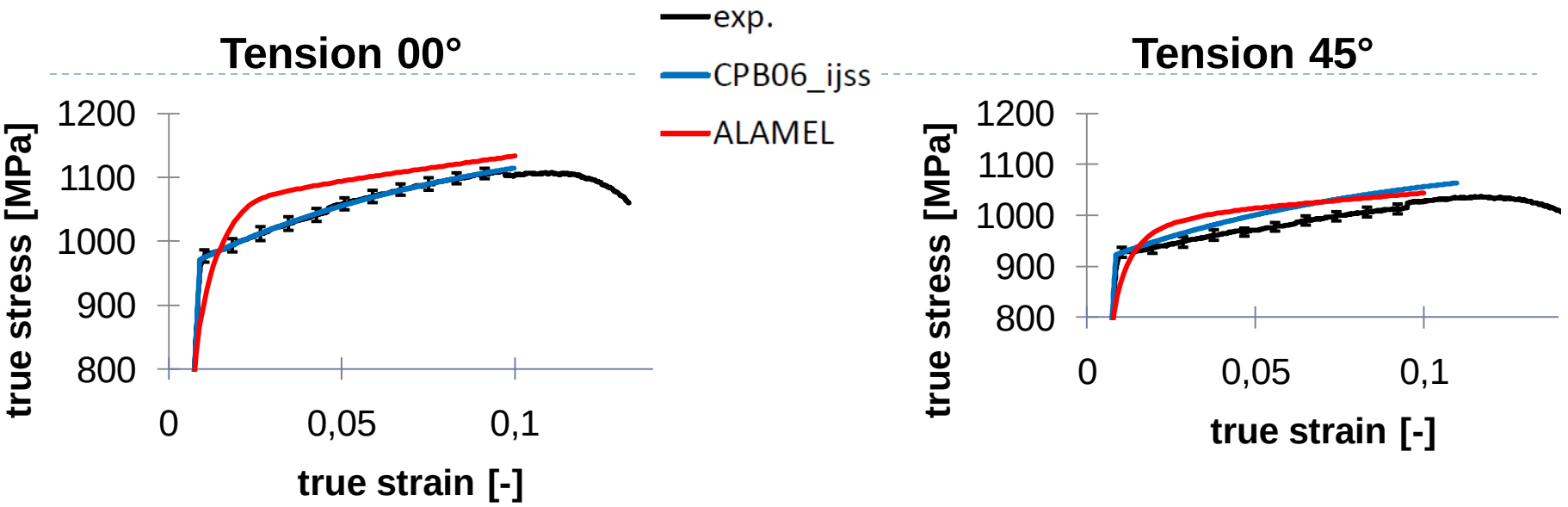

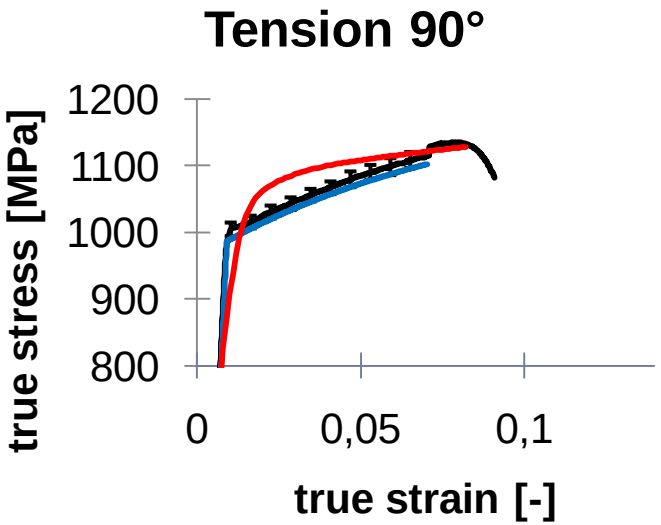

No texture hardening by crystal plasticity prediction

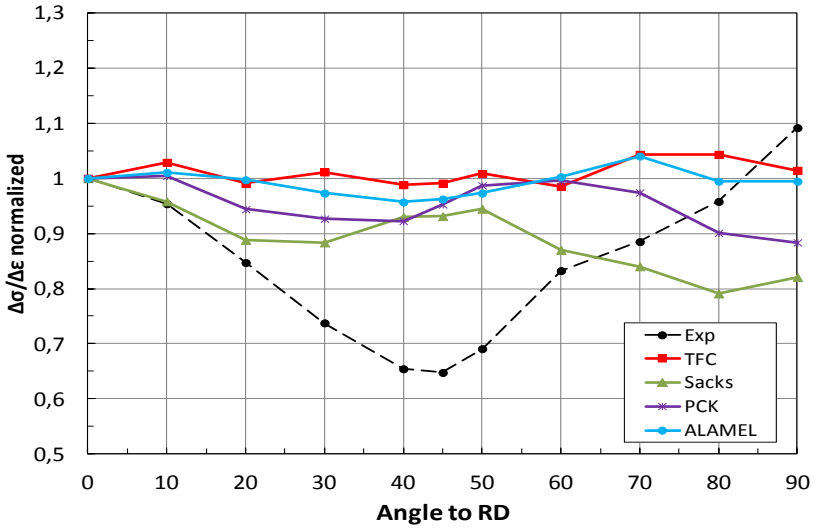

Elastic Plastic transition ALAMEL // Exper.

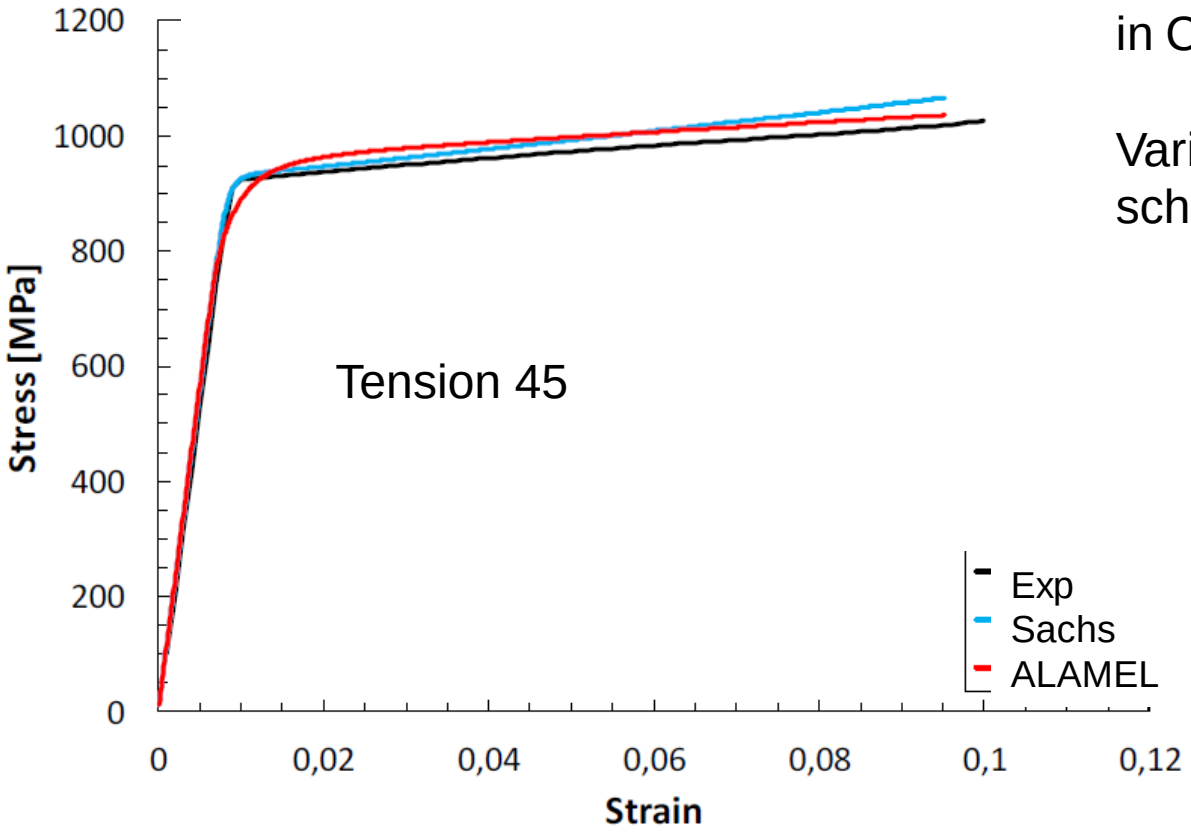

Variation of hardening function in CRSS model : no effect

Variation of homogenization scheme :

Sachs or ALAMEL
Strong effect

Experiments :
sharp transition
all grains
simultaneously plastify

→ Sachs assumption good for EP transition

Comparison Cazacu // Lamel // Experiments

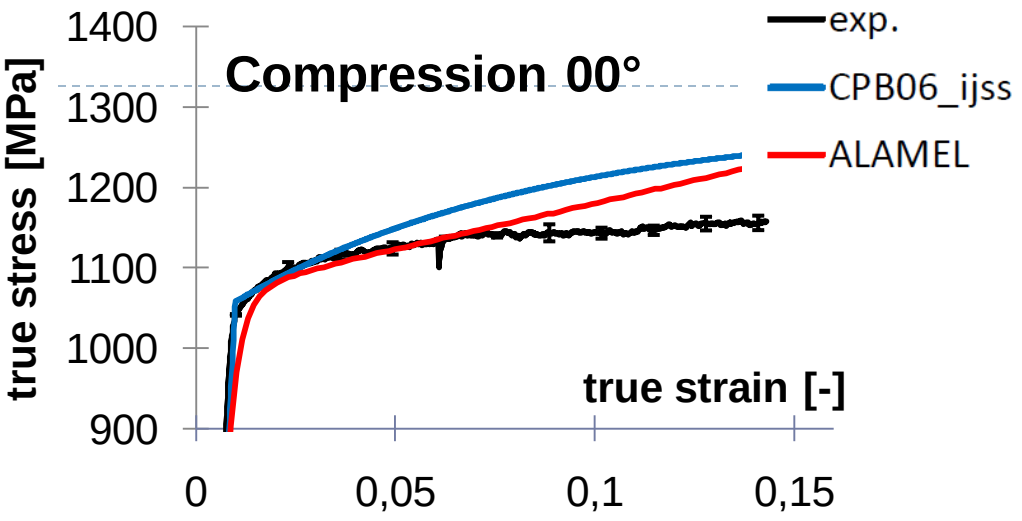

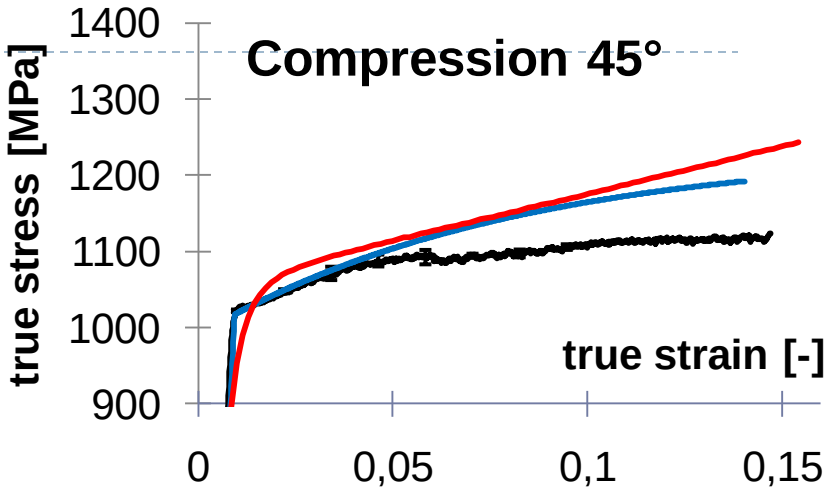

ALAMEL not identified on compression but good prediction yield point bad in hardening

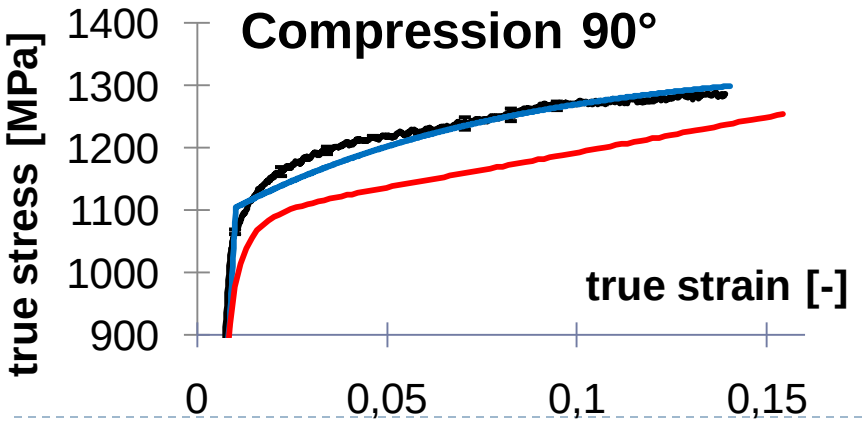

Layer compression tests

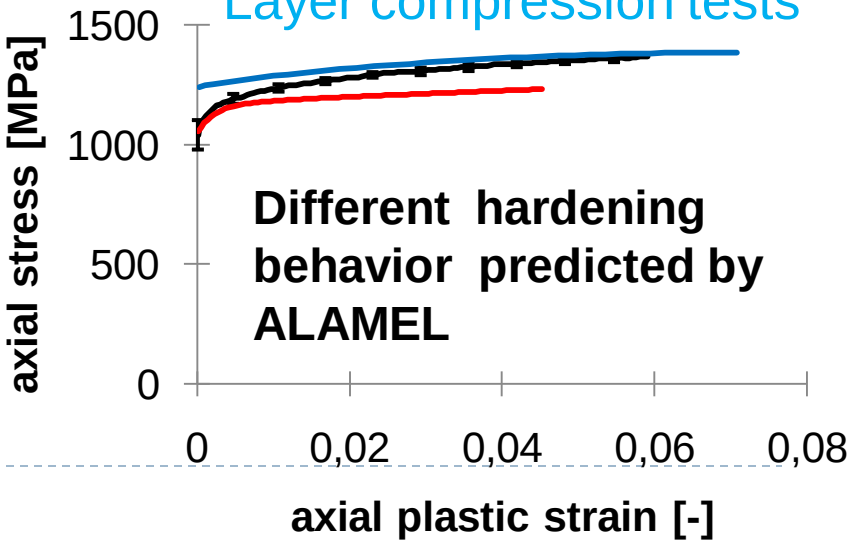

Comparison Cazacu // Lamel // Experiments

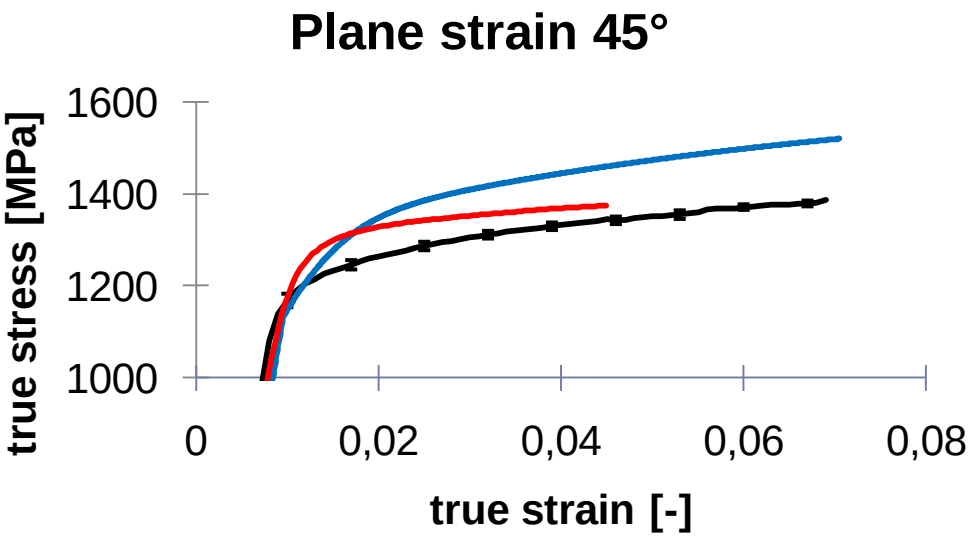

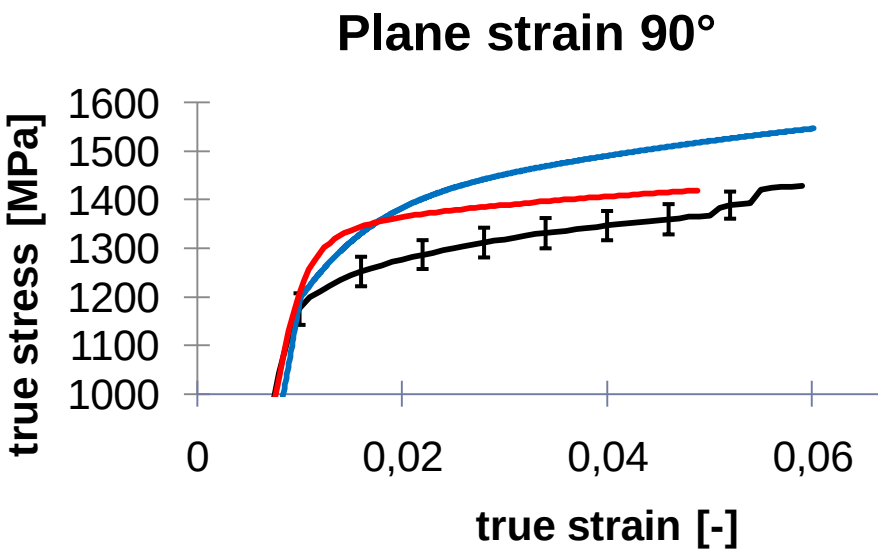

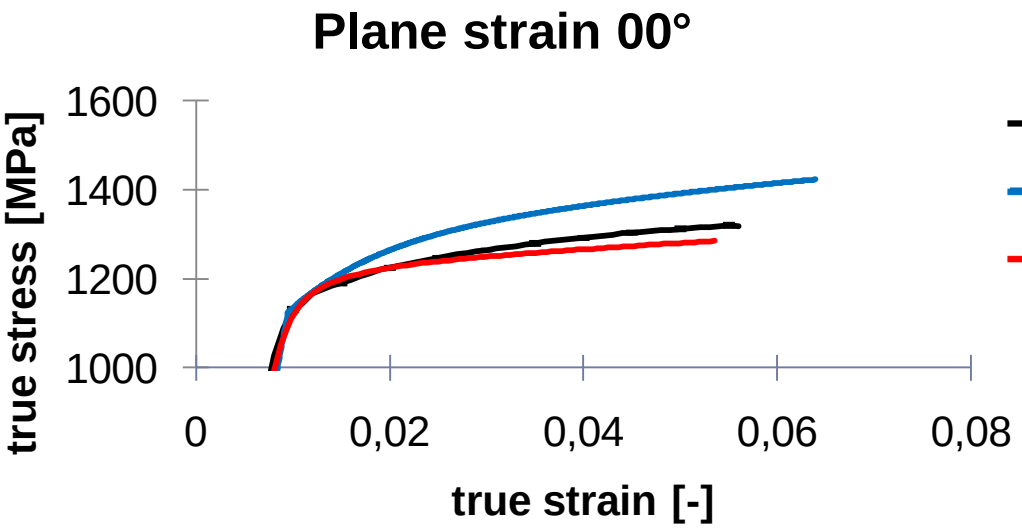

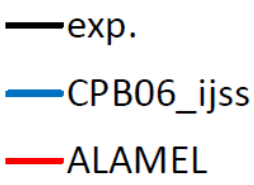

ALAMEL identified as IJSS on tensile tests
able to predict Plane Strain better than IJSS

Comparison Cazacu // Lamel // Experiments

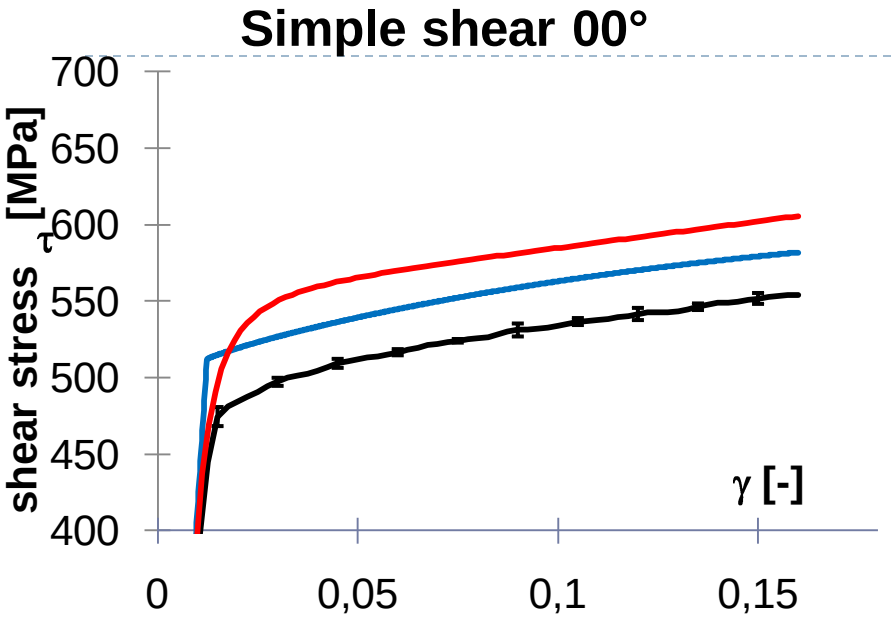

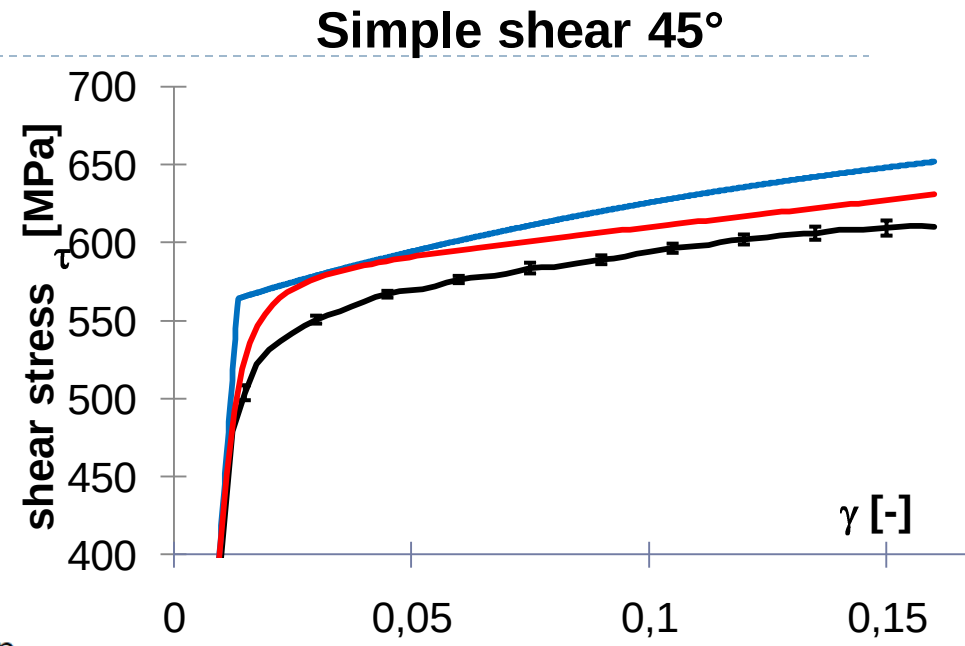

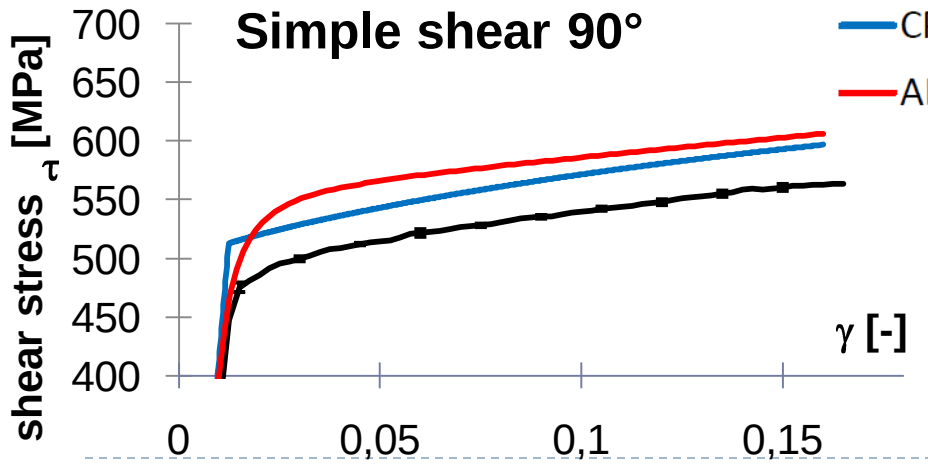

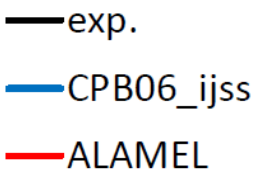

For shear ALAMEL less efficient

How to explain different efficiency of ALAMEL depending on strain paths ?

-homogeneity rule preventing good modeling of yield entrance (Sachs // Taylor // ALAMEL…)

-lack of accuracy on CRSS hardening:
single function applied on an equivalent shear,
no latent hardening

-texture evolution → texture hardening behavior but no twinning effect

→ Analysis of texture evolution, activated slip systems…

Analysis of ALAMEL results

-predicted and experimental hardening slope,

-predicted slip system activity,

-experimental and predicted texture evolution

-order and magnitude of experimental and predicted curves by ALAMEL

→ **Pyramidal slip systems are the most active ones**

→**Twinning not important in this sheet**

2 % twins in shear tests in 45 = 0 when 1% twins in shear test at 90 both experiments and predictions gives O =90 similar stress-strain curve

→ **Assumption of**

→Too low CRSS hardening for pyramidal slip systems

→Too high CRSS hardening for basal and prismatic slip systems could explain different efficiency of the model depending on strain path

Conclusions and Perspectives

Good potential of Cazacu and ALAMEL
Material set of parameters available

Accurate identification of Cazacu requires more tests in the data base
can lead to different behavior according chosen tests
(Bi axial points in tensile and compression are key data !!)
ALAMEL can help CAZACU

Perspectives with ALAMEL:

- different hardening for different slip systems + latent hardening
- application on other Ti_6Al_4V : promising
- twinning model

with Cazacu:

- improve model hardening

Acknowledgement

Interuniversity Attraction Poles Programme
Belgian Science Policy (Contract P7/21).

The Belgian Fund for Scientific Research FRS-FNRS

Validation by a cup deep drawing test

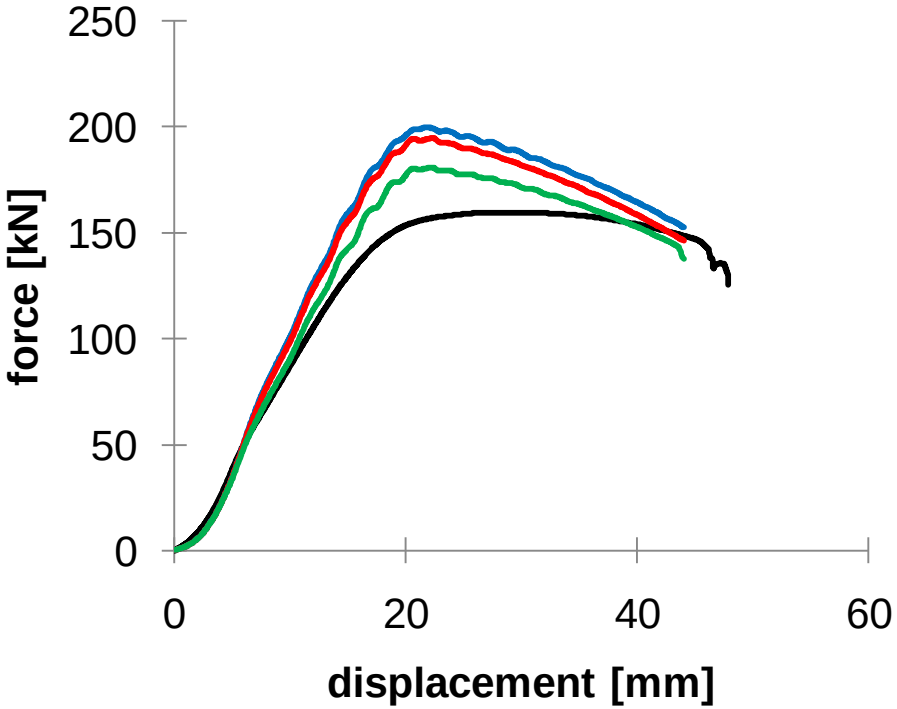

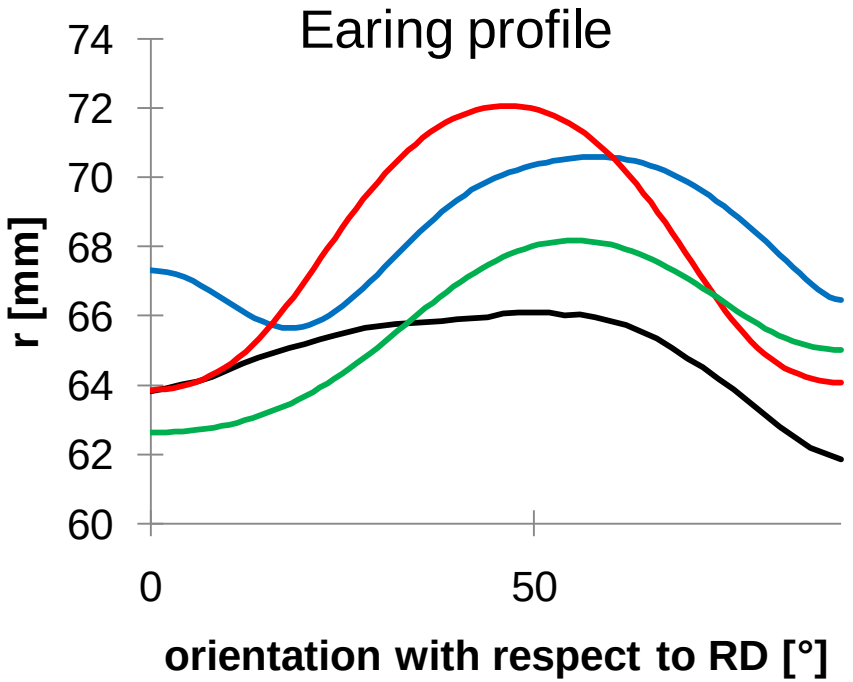

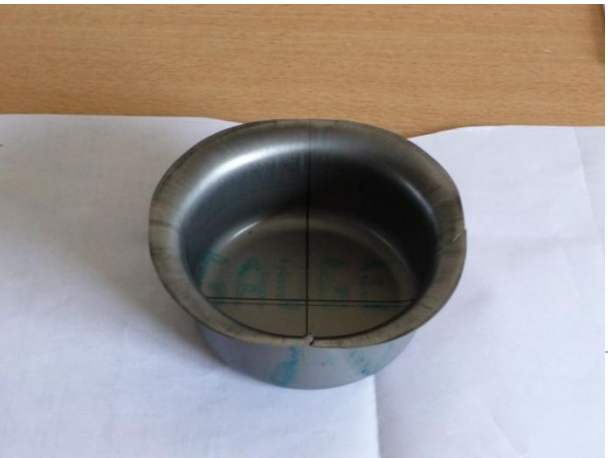

Finally **new a2** more accurate for cup deep drawing…

Remind new a2 the closest for global test results in Plane stress state…

exp.
CPB06_ijss
CPB06_iutam
CPB06_new_a2

Compression test at constant strain rate

SCHENCK Hydropuls 400 kN press

Specimen

System 1

System 3

System 2

Experimental set-up (DIC)

Tensile samples for texture measurements

X-Ray Diffraction at mid- thickness on specimens deformed up to 5% & ~10%

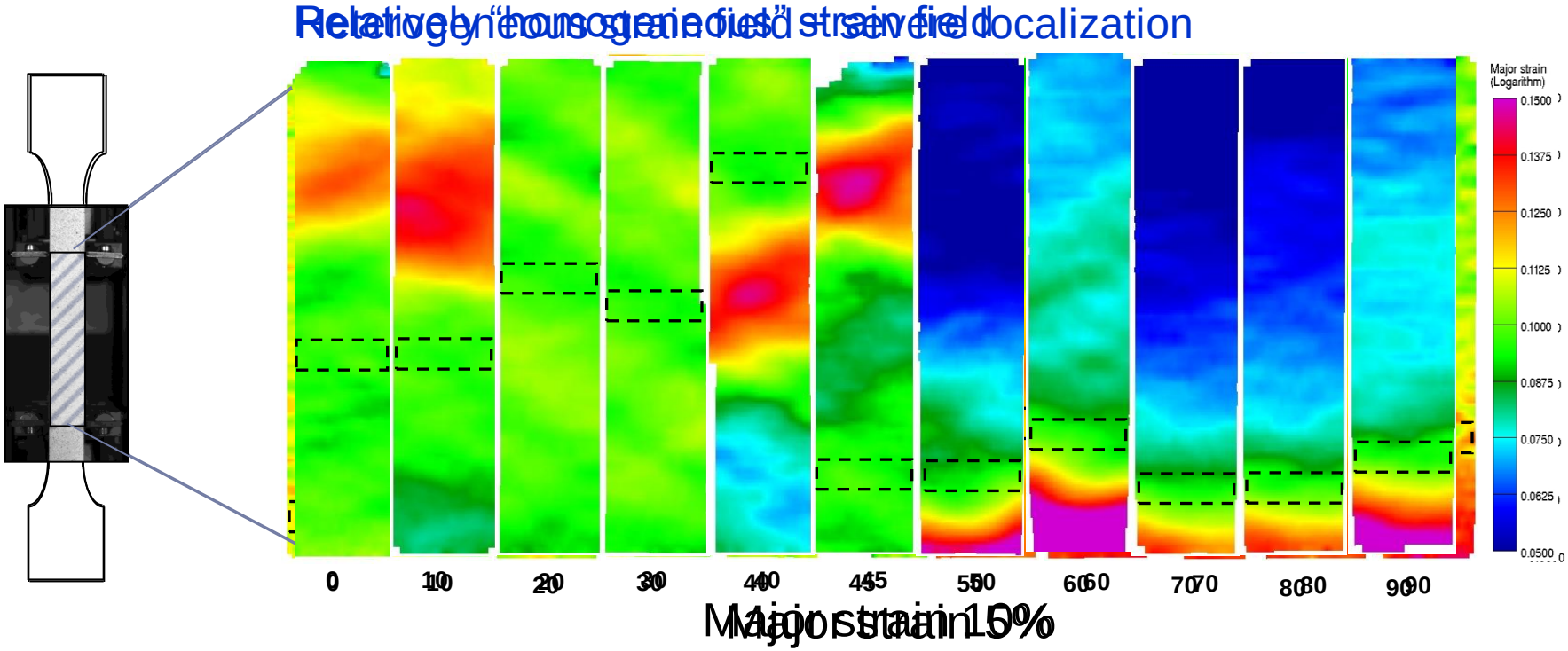

Activated slip systems in tensile

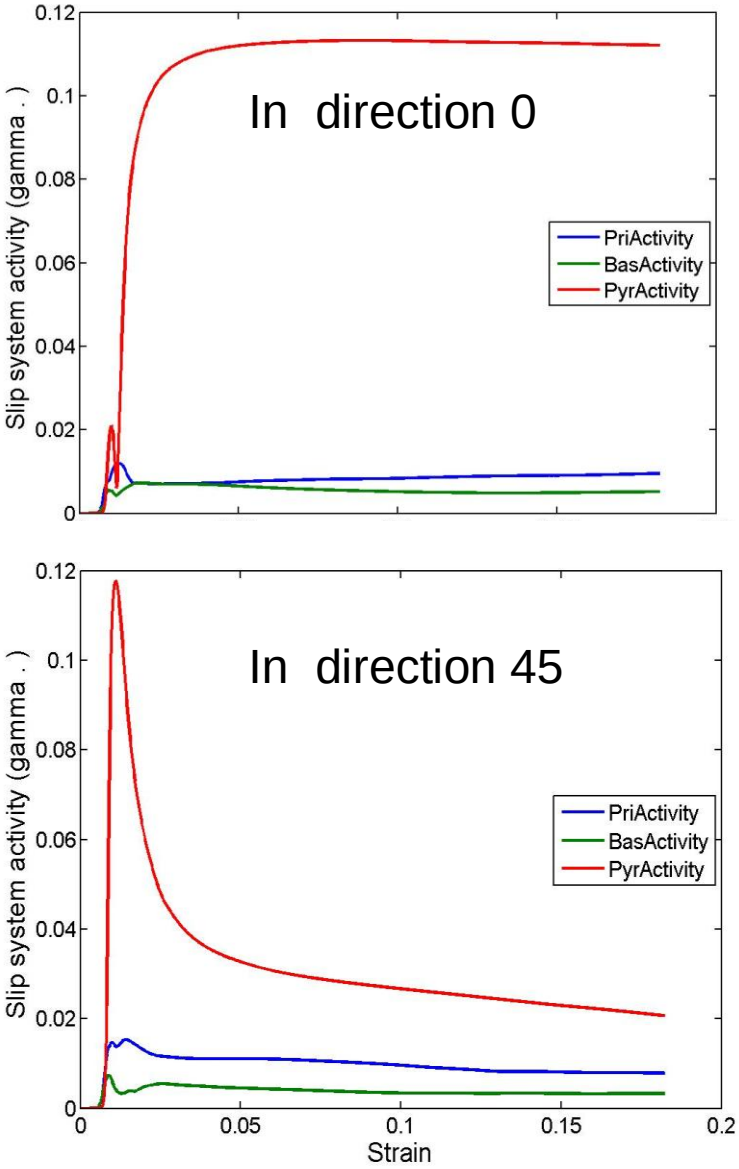

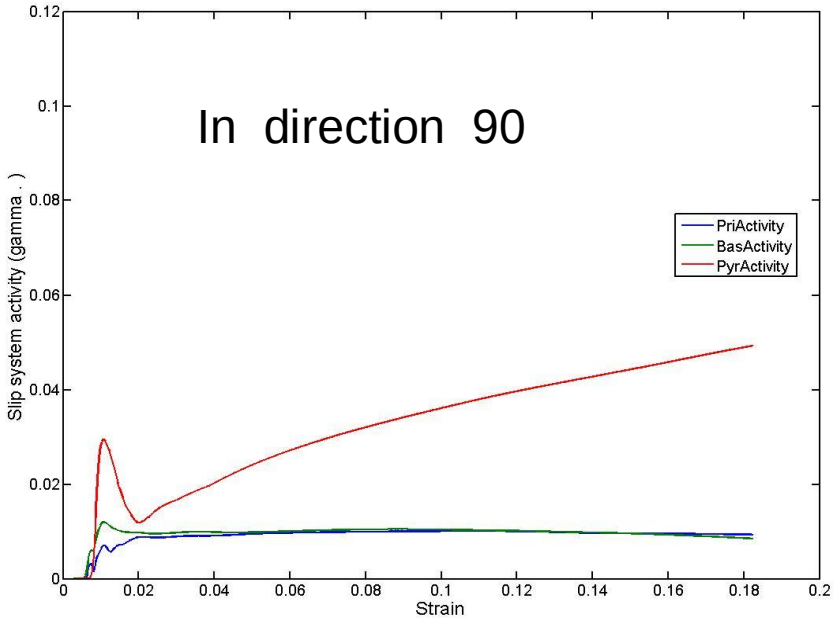

Activated slip systems in compression

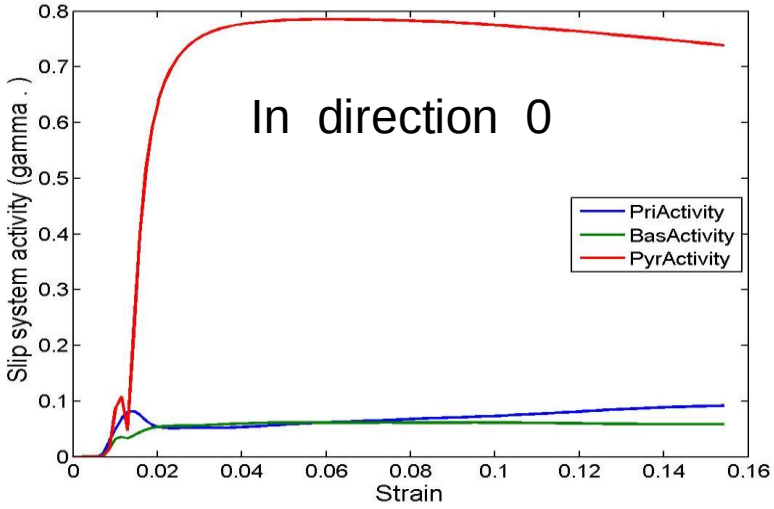

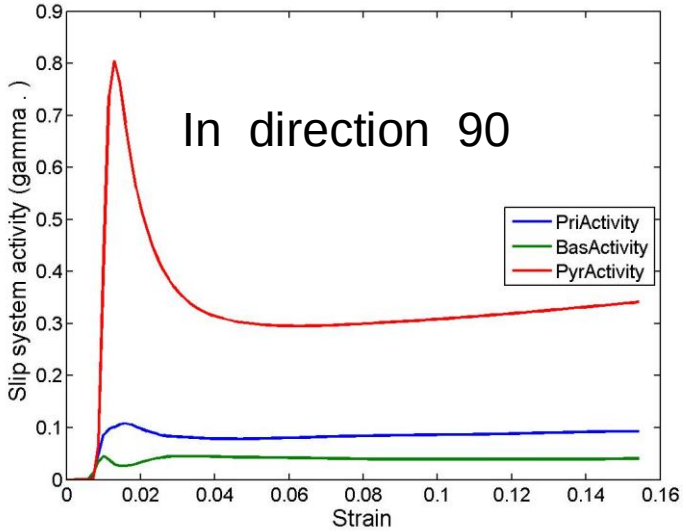

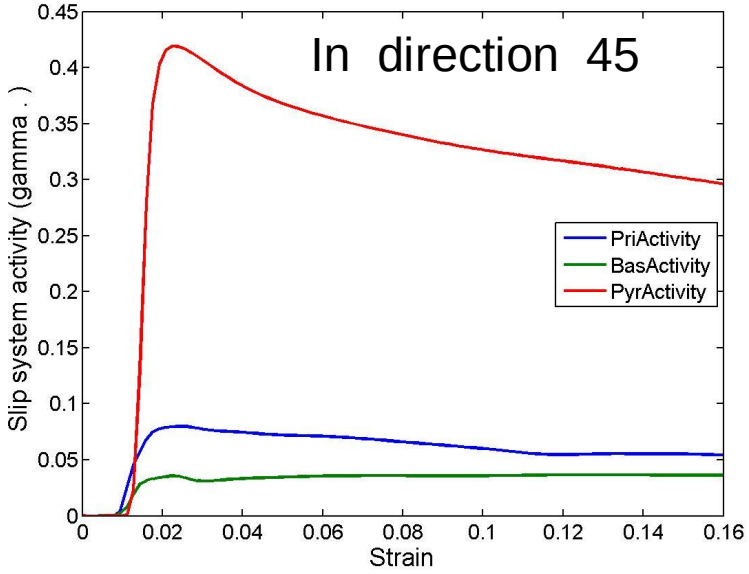

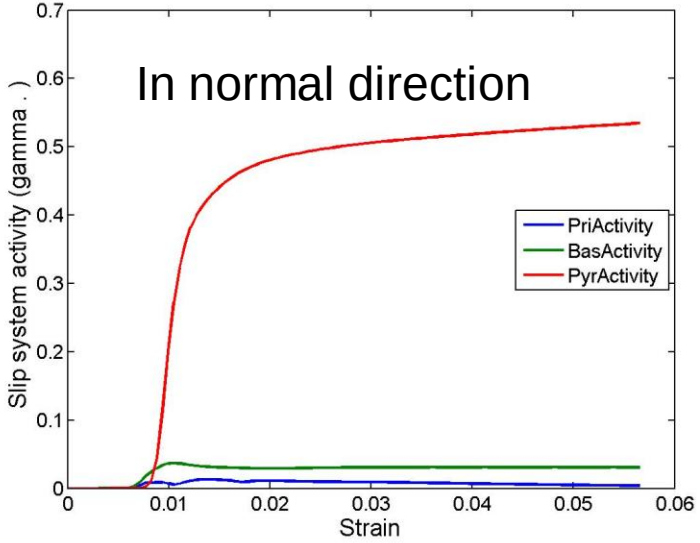

Activated slip systems in plane strain

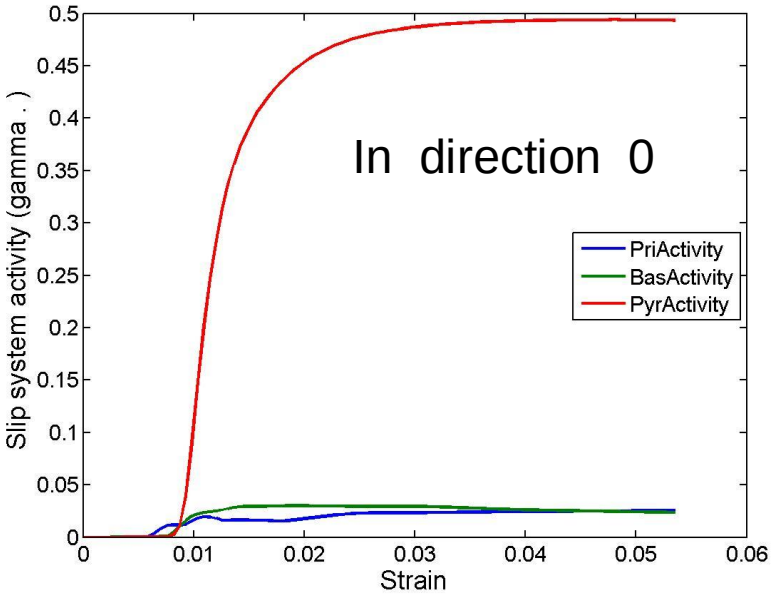

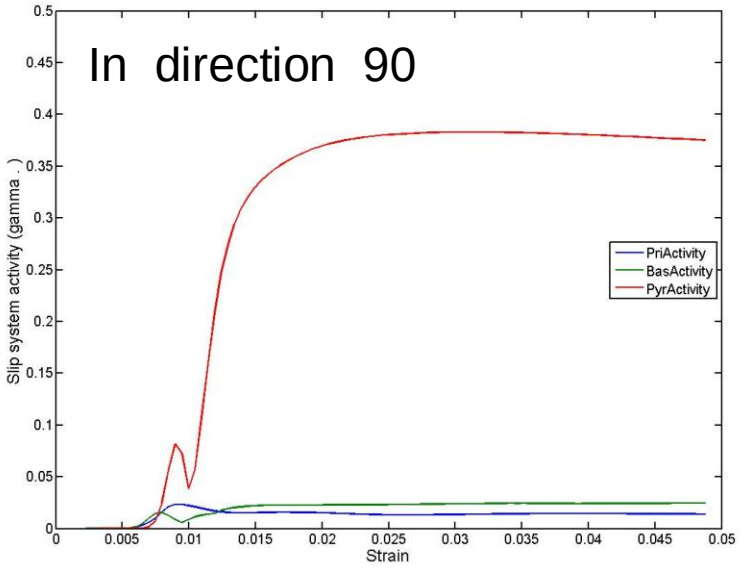

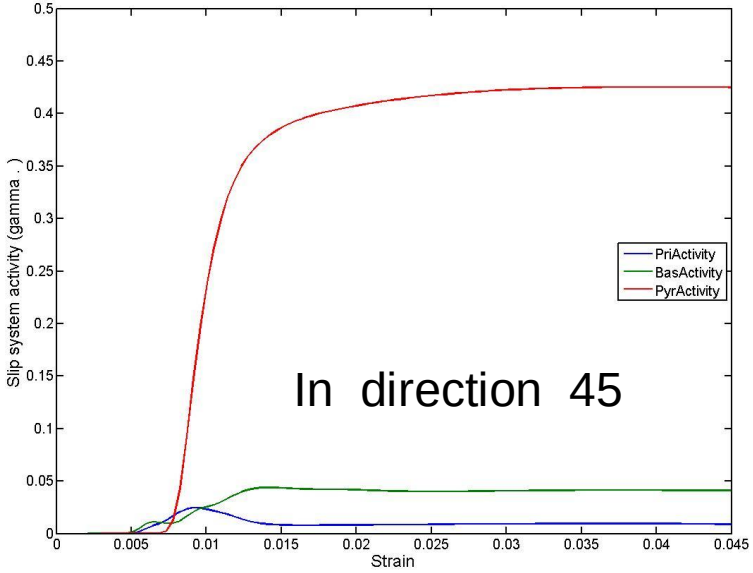

Activated slip systems in shear

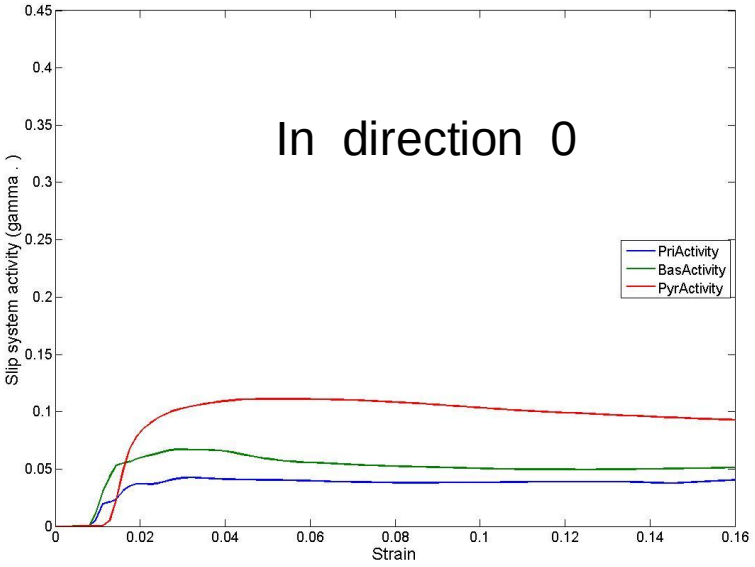

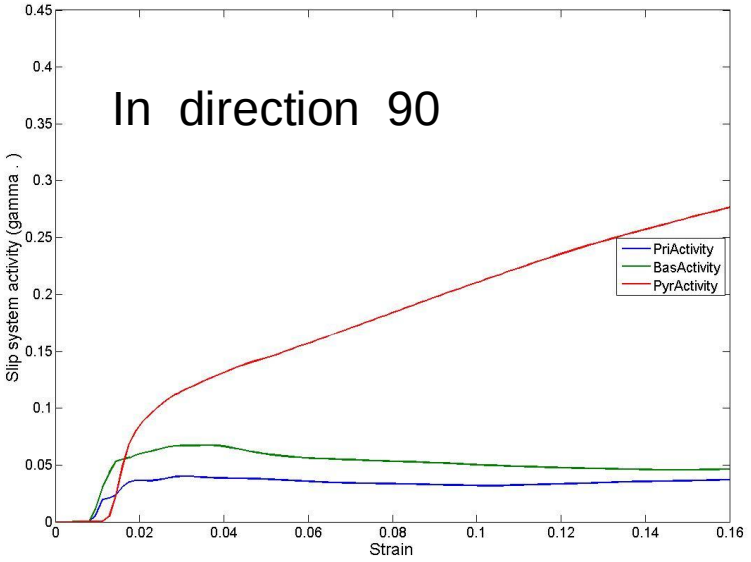

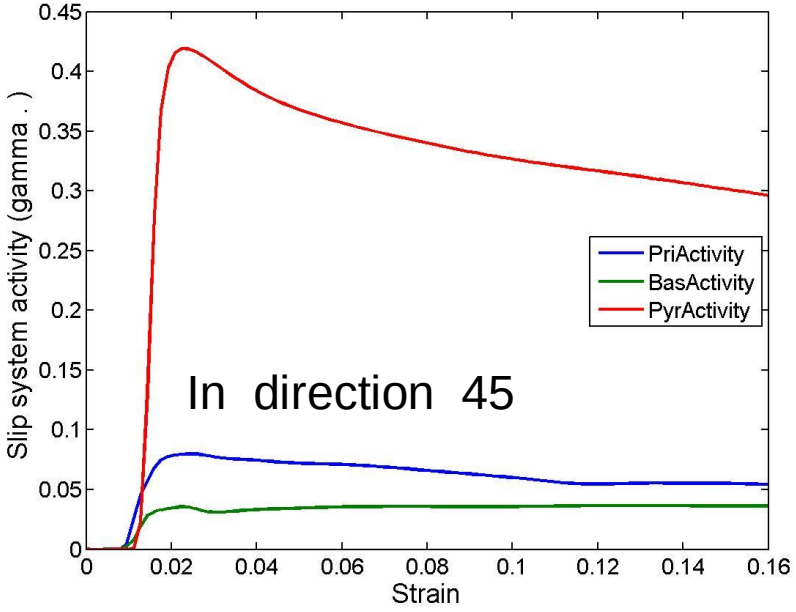

Evolution of C axis in compression

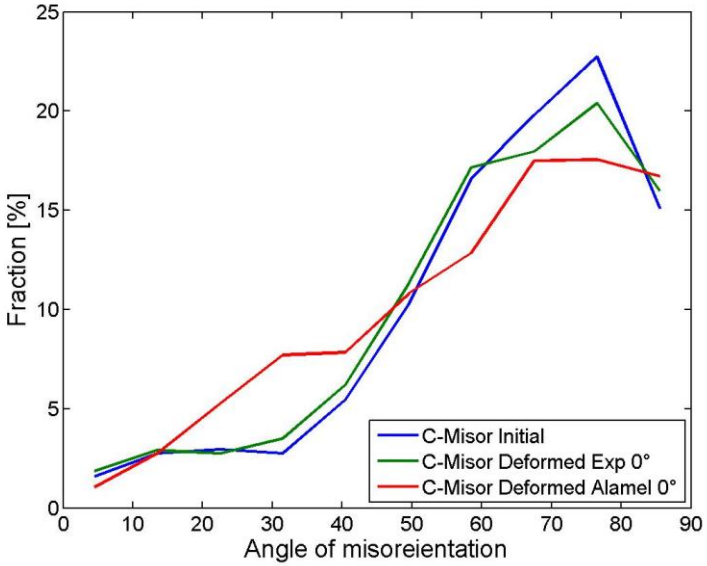

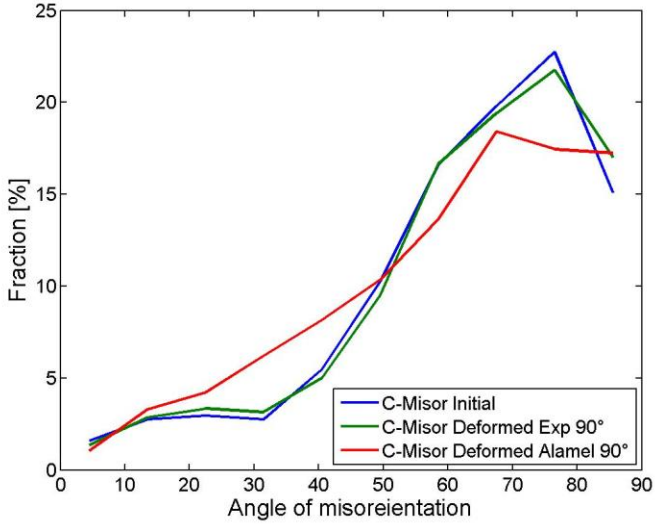

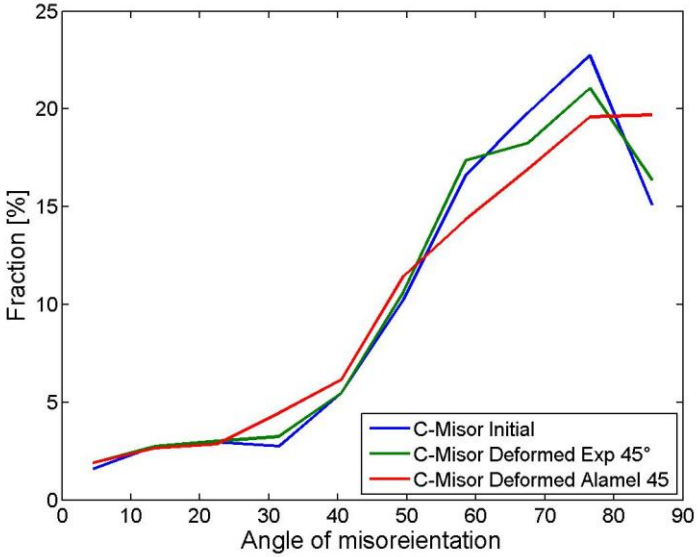

C axis in tensile plane strain

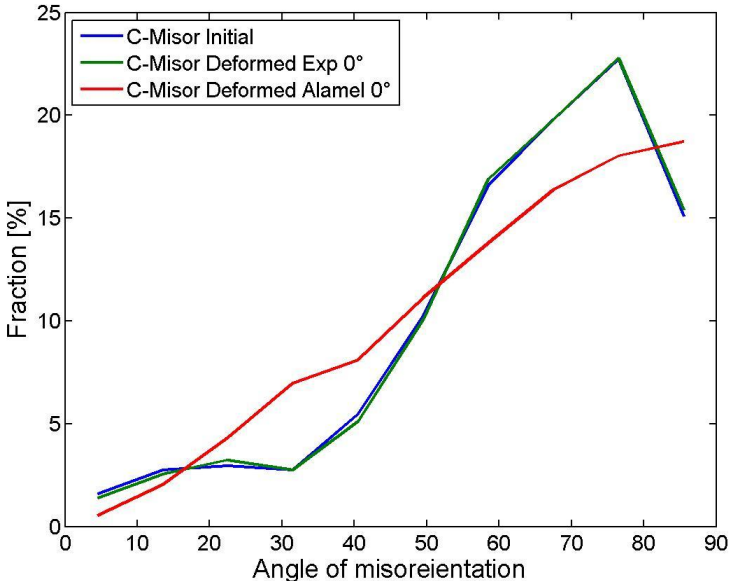

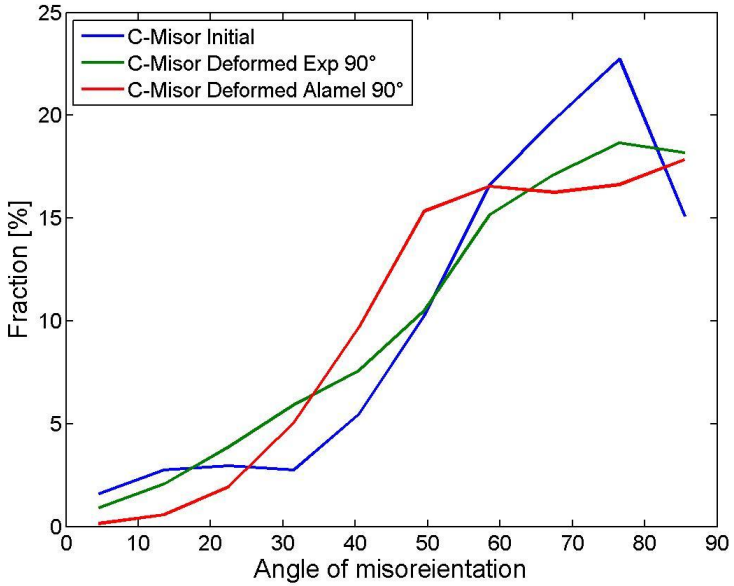

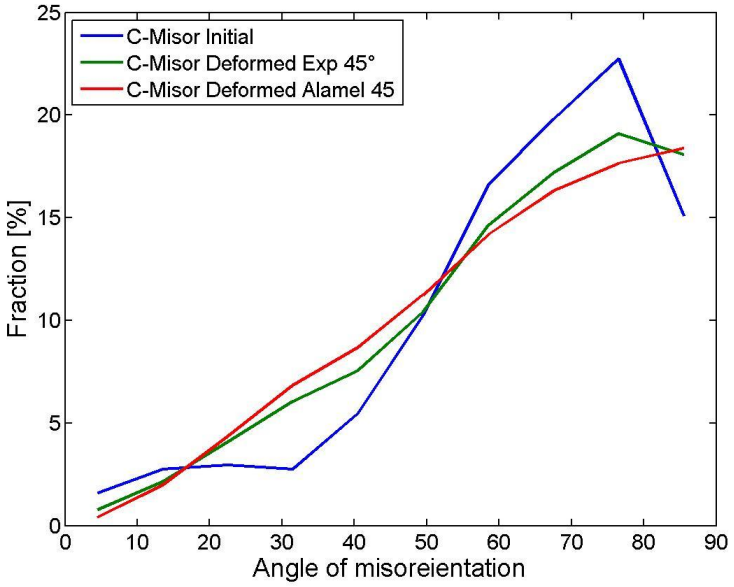

Evolution of C axis in shear

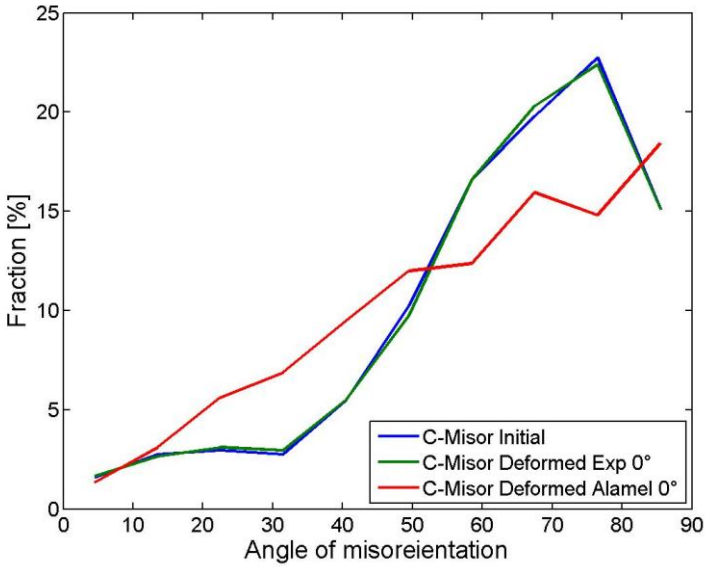

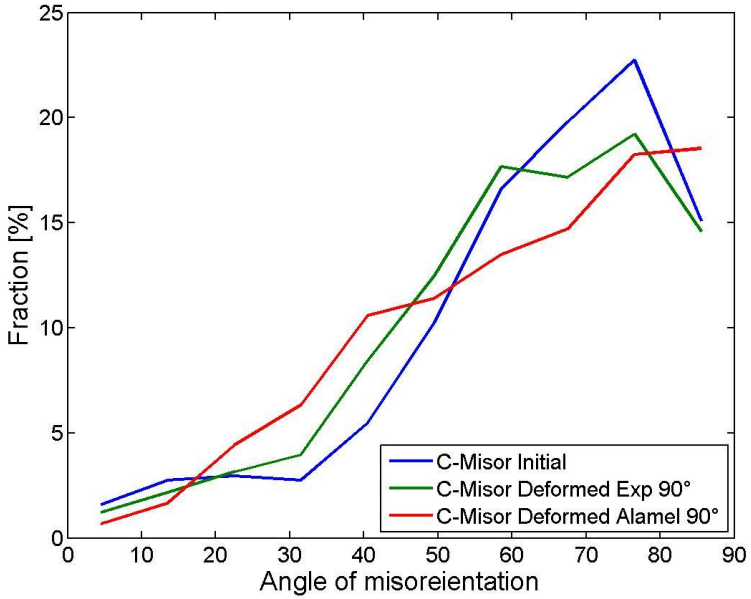

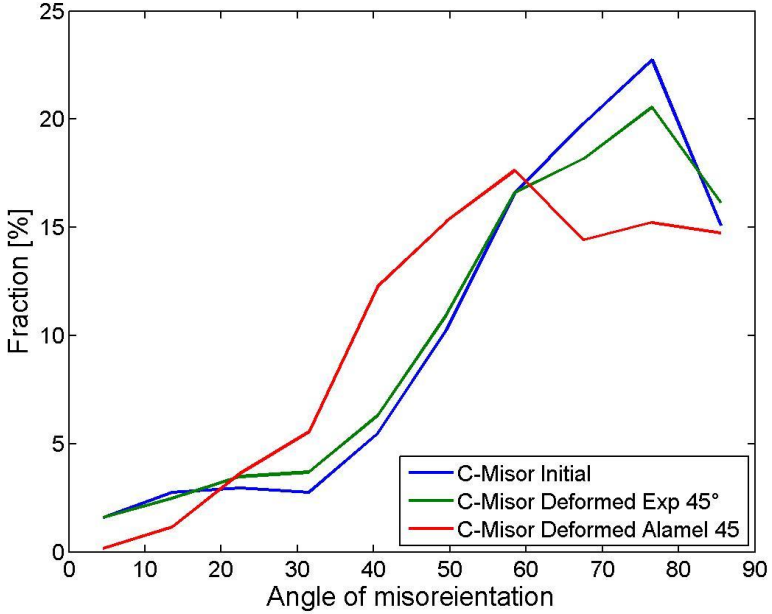

Mid-thickness crystallographic aspect

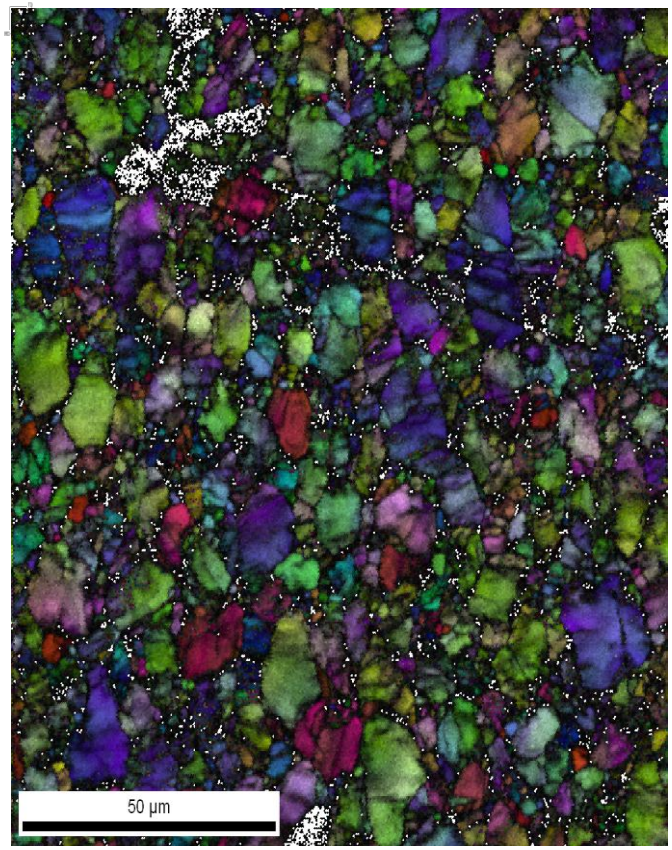

Non re-crystallized material

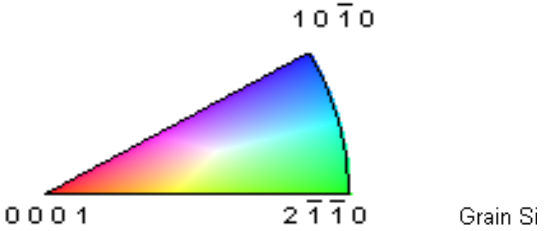

Alpha phase: 88.2%

Beta phase: 9.3%